Economic Geology, v. 106, pp. 331–358

A Carbonaceous Sedimentary Source-Rock Model for Carlin-Type and Orogenic Gold Deposits

Ross R. Large,[1,†] Stuart W. Bull,[1] and Valeriy V. Maslennikov[2]

[1] *CODES ARC Centre of Excellence in Ore Deposits, University of Tasmania, Private Bag 126, Hobart, Tasmania, Australia 7001*

[2] *Institute of Mineralogy, Russian Academy of Science, Urals Branch, Miass, Russia*

Abstract

This paper presents evidence and arguments that carbonaceous sedimentary rocks were a source for Au and As in sediment-hosted orogenic and Carlin-type gold deposits and develops a corresponding genetic model. In this two-stage basin-scale model, gold and arsenic are introduced early into black shale and turbidite basins during sedimentation and diagenesis (stage 1) and concentrated to ore grades by later hydrothermal, structural, or magmatic processes (stage 2). In reduced continental margin basin settings, organic matter, sedimented under anoxic to euxinic conditions, immobilizes and concentrates gold, arsenic, and a range of trace elements (particularly V, Ni, Se, Ag, Zn, Mo, Cu, U) present in marine bottom waters, into fine-grained black mudstone and siltstone of slope and basin facies. During early diagenesis, gold and certain other trace elements (Ni, Se, Te, Ag, Mo, Cu, ±PGE) are preferentially partitioned into arsenian pyrite that grows in the muds. These processes produce regionally extensive black shale and turbidite sequences enriched in syngenetic gold and arsenic, commonly from 5 to 100 ppb Au and 10 to 200 ppm As. Rare organic- and sulfide-rich metalliferous black shales may contain up to 1 to 2 ppm Au and over 1,000 ppm As, present as refractory gold in arsenian pyrite and nanoparticles of free gold.

During late diagenesis and early metamorphism (stage 2) the diagenetic arsenian pyrite is recrystallized to form coarser grained pyrite generations, and the organic matter is cooked to bitumen. Under higher grade metamorphism (lower greenschist facies and above) arsenian pyrite in carbonaceous shales is converted to pyrrhotite. These processes release gold, arsenic, sulfur and other elements (Sb, Te, Cu, Zn, Mo, Bi, Tl, and Pb) from the source rocks to become concentrated by hydrothermal processes, locally to produce gold ores, in structural sites such as fold hinge zones, shear or breccia zones within or above the black shale sequence.

LA-ICP-MS analyses of diagenetic pyrite in carbonaceous sediments, both associated and not associated with gold deposits, suggests that invisible gold contents of greater than 250 ppb in diagenetic pyrite, are indicative of carbonaceous shale source rocks with the potential to produce economic gold deposits. Application of this sedimentary source-rock model enables a systematic exploration approach for sediment-hosted gold deposits, based on the distribution, composition and structure of carbonaceous shale sequences and their contained diagenetic pyrite.

Introduction

This investigation sought to determine whether, or not, carbonaceous sedimentary rocks could have been an important source for gold in orogenic and Carlin-type gold deposits. Development of the resulting model has been stimulated by an industry collaborative AMIRA International research project (Large et al., 2007, 2009; Chang et al., 2008; Meffre et al., 2008; Scott et al., 2008), combined with previous ideas on gold ore genesis presented by Boyle (1979), Buryak (1982), Kribek (1991), Titley (1991), Hutchinson (1993), Cooke et al. (2000), Hofstra and Cline (2000), Emsbo (2000), Reich et al. (2005), and Wood and Large (2007). Our research has been focused on Sukhoi Log (Siberia), Bendigo (Victoria), and the northern Carlin Trend (Nevada) but also includes data from Spanish Mountain (British Columbia), Macraes (South Island New Zealand), and Kumtor (Kyrgyzstan).

Although there is some consensus on aspects of the models for orogenic and Carlin-type gold deposits, there remains a number of unresolved questions (Groves et al., 2003; Cline et al., 2005). The model presented here challenges three current views related to orogenic gold deposits: (1) gold-rich fluids are derived from deep metamorphic processes or from crustal granites—we contend the gold is sourced in the sedimentary basin; (2) organic-rich sediments are traps for gold—we contend that organic-rich sediments are excellent source rocks for gold and a variety of other elements (As, Zn, V, Mo, Ag, Ni, Se, Te); and (3) gold is introduced late, i.e., syn- or posttectonic—we contend that gold is introduced early (syndiagenetic) and remobilized and concentrated locally on a scale of meters to kilometers during syntectonic and/or synmagmatic fluid flow.

The gold ores under consideration have been variously categorized as orogenic, turbidite-hosted, and Carlin-type gold deposits. They are strata bound and discordant to bedding, comprised of disseminated pyrite (±arsenopyrite and pyrrhotite) concentrated in black shale, siltstone, carbonate, and sandstone sequences (Table 1; Figs. 1, 2). Some of the world's largest gold districts and/or deposits are of this type (e.g., Muruntau, Ashanti, northern Carlin Trend, Kumtor, Homestake, Sukhoi Log; Table 1). Quartz veining may or may not be present (Fig. 2). Gold may be refractory (dissolved within arsenian-pyrite or arsenopyrite) or, in the case of many deposits, occurs as free gold or gold tellurides within metamorphic and/or hydrothermal pyrite, arsenopyrite, or associated quartz veins. The key criteria for considering this diverse group of deposits together is that they are hosted by sedimentary rocks and, in particular, carbonaceous mudstones or shales make up a significant component of the sedimentary

† Corresponding author: e-mail, Ross.Large@utas.edu.au

Submitted: August 3, 2010
Accepted: January 11, 2011

TABLE 1. Some Major Sediment-Hosted Gold-Arsenic Deposits and Districts (modified after Goldfarb et al., 2005)

Deposit	Location	Au (t)	Au grade (g/t)	Age of host rocks	Sedimentary lithologic units
Alaska-Juneau	U.S. Cordilera	281	1.4	Late Jurassic-Early Cretaceous	Metasediments
Macreas Flat	New Zealand	251	1.2	Jurassic	Carbonaceous schists
Spanish Mountain	Western Canada	54	0.8	Triassic	Carbonaceous mustone, graywacke
Natalka	Russian Far East	716	4.2	Permian	Carbonaceous mustone, sandstone
Nezhdaninskoye	Russia	311	5.4	Early Permian	Carbonaceous siltstone, sandstone
Bakyrichik	Tien Shan Asia	361	6.8	Carboniferous	Carbonaceous metasediments
Carlin Trend	Nevada	3000	0.9 to 19	Siluro-Devonian	Calcareous carbonaceous mustone, limestone
Zarmitan	Tien Shan Asia	470	9.5	Silurian	Metasediments
Muruntau	Tien Shan Asia	5290	3.5-4.0	Ordovician-Silurian	Carbonaceous mustone, carbonate, sandstone
Amantaitau	Tien Shan Asia	288	3.7	Ordovician-Silurian	Carbonaceous metasediments
Bendigo	SE Australia	533	12.9	Lower Ordovician	Sandstone, carbonaceous mudstone
Getchell district	Nevada	800	3	Cambro-Ordovician	Calcareous carbonaceous mustone, limestone
Sukhoi Log	Edge Siberian craton	1920	2.8	Neoproterozoic	Carbonaceous mudstone, siltstone
Kumtor	Tien Shan Asia	284	4.4	Neoproterozoic	Mudstone, siltstone, sandstone
Telfer	Patterson, WA	1564	1.5	Neoproterozoic	Sandstone, mudstone
Olimpiada	Edge Siberian craton	700	10.9	Neoproterozoic	Schists, carbonaceous slates
Brasilia	Brazil	313	0.4	Neoproterozoic	Carbonaceous phyllite
Ashanti	West AfriCa	2070	4.7	Paleoproterozoic	Metasediments
Homestake	Trans-Hudson USA	1237	8.3	Paleoproterozoic	BIF, metasediments
Granites-Tanami	Central Australia	369	4.6	Paleoproterozoic	Metasediments, BIF

succession (Figs. 1, 2). For the orogenic deposits of this group, metamorphism and deformation have been critical processes in their genesis. In contrast, although deformation has been important in the genesis of Carlin-type deposits, the ores have formed in rocks of low metamorphic grade. Our view is that carbonaceous sediment-hosted gold deposits can form in a diverse range of environments from very low grade diagenetic to metamorphic (archizone) environments to moderate (green schist) metamorphic environments. Deposits in higher grade rocks (amphibolite and granulite facies) have

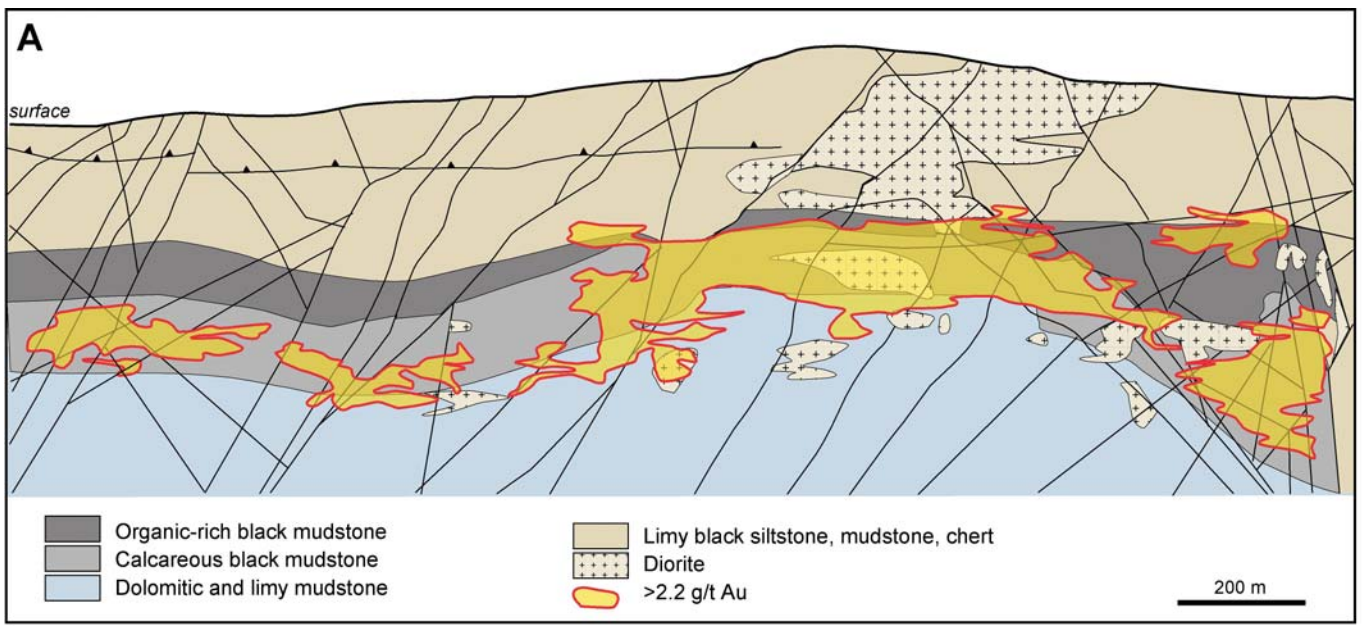

FIG. 1. Typical geologic cross sections showing relationship of carbonaceous sediments to orebodies in selected gold deposits. A. Betze-Post deposit, northern Carlin Trend (Bettles, 2002). Pyritic gold ores in yellow are strata bound and structurally controlled in the Popovich Formation. B. Sukhoi Log, Lena gold district (Wood and Popov, 2006). Pyritic gold ore is concentrated in an overturned anticline in carbonaceous shales and siltstones. C. Bendigo, central Victoria (Willman, 2007). D. Dufferin deposit, Meguma district (Ryan and Smith, 1998). Gold ores occur in quartz-rich saddle reefs and associated crosscutting quartz veins.

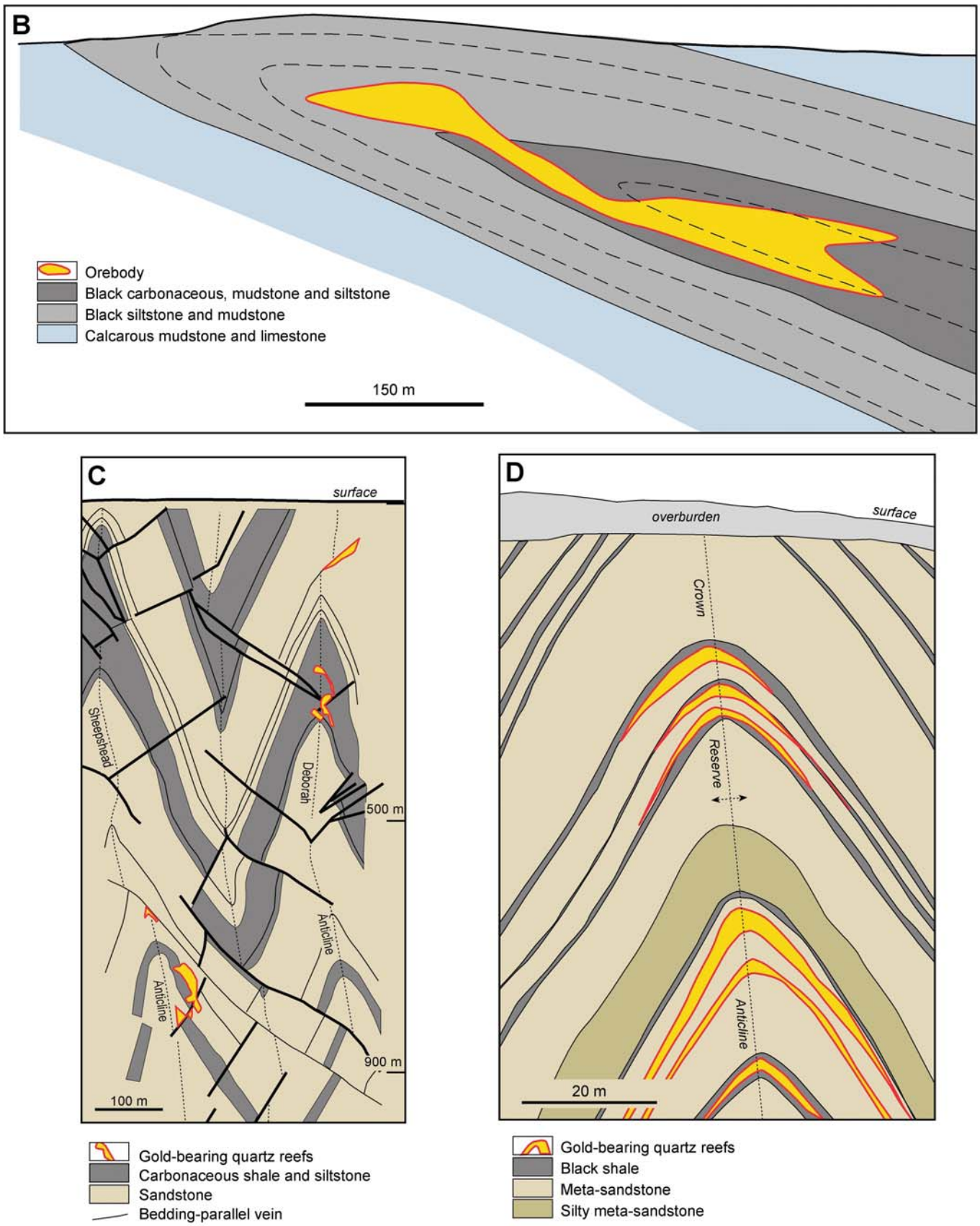
B
Orebody
Black carbonaceous, mudstone and siltstone
Black siltstone and mudstone
Calcarous mudstone and limestone
150 m
C
surface
Sheepshead
Deborah
Anticline
Anticline
500 m
900 m
100 m
Gold-bearing quartz reefs
Carbonaceous shale and siltstone
Sandstone
Bedding-parallel vein
D
overburden
surface
Crown
Reserve
Anticline
20 m
Gold-bearing quartz reefs
Black shale
Meta-sandstone
Silty meta-sandstone

FIG. 1. *(Cont.)*

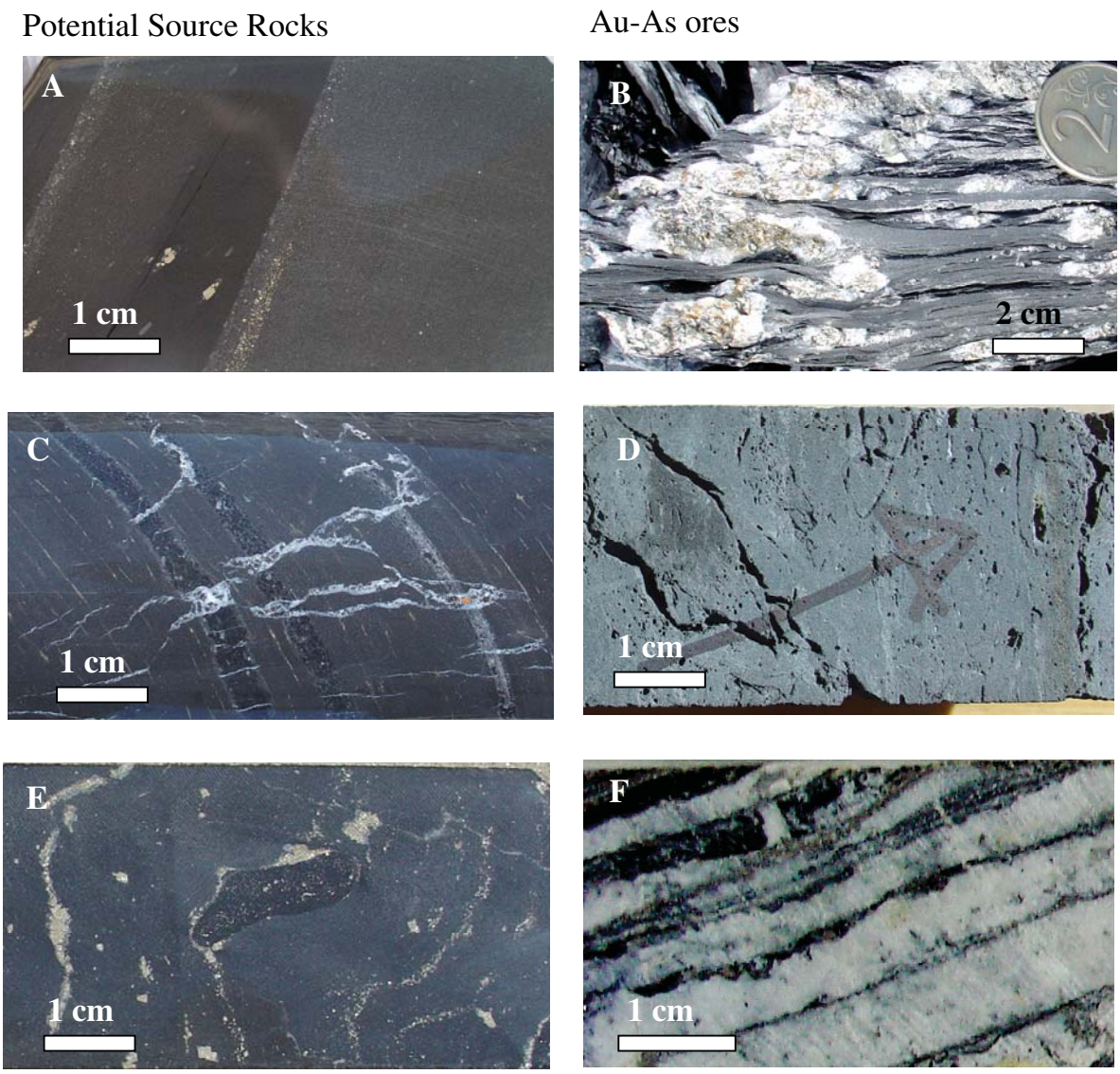

FIG. 2. Carbonaceous shales and related gold-arsenic ores. A. Sukhoi Log pyritic carbonaceous mudstones and siltstones of the Khomolkho Formation, considered as the source rocks for the deposit. B. Folded gold-bearing pyrite-quartz veinlets emplaced during deformation of carbonaceous shale source rocks at Sukhoi Log. C. Popvich Formation pyritic carbonaceous mudstone, with calcite-bitumen veins, from the Upper Mud Member. D. Decalcified carbonaceous mudstone with high-grade Au-As mineralization, Popovich Formation at Goldstrike, Carlin. E. Bendigonian pyritic carbonaceous shale, host to the gold saddle reefs. F. Bedding-parallel laminated quartz vein in the foot zone of a gold-rich saddle reef, Bendigo mine.

most likely been metamorphosed postgold mineralization (e.g., Tomkins and Grundy, 2009). Greenstone-hosted orogenic gold deposits are not included in this discussion, although the gold source rocks may include black shales (Tompkins, 2010).

The features of these deposits have been exhaustively covered by previous workers (see Boyle, 1986; Cooke et al., 2000; Hofstra and Cline, 2000; Cline et al., 2005; and Goldfarb et al., 2005, for thorough reviews) and will not be elaborated further here. In some cases, carbonaceous mudstones and siltstones are the dominant host rock (e.g., Sukhoi Log, Bakyrchik, Brasilia, and Kumtor) or make up only a part of the host stratigraphy, forming the tops to fining-upward turbidite cycles (e.g., Victorian and Meguma provinces). In other cases, carbonaceous carbonate rocks predominate (e.g., the Popovich and Roberts Mountain Formations in the northern Carlin Trend).

Preenriched Source Rocks: Marine Carbonaceous Mudstones, and Shales

Many models for orogenic and Carlin-type gold deposits consider that the source of gold is at depth, well below the deposits; for example, the mantle (e.g., Perring et al., 1987; Barley and Groves, 1990), deep crust at amphibolite or granulite facies (Kerrich and Fryer, 1979; Phillips et al., 1987; Cline et al., 2005; Kerrich et al., 2005), deep siliciclastic rocks (Ilchik and Barton, 1997), or from deep magmas (e.g., Burrows and Spooner, 1985; Spooner, 1993; Johnston and Ressel, 2004,

Muntean et al., in press). However, before the development of these models, the concept that gold was sourced from the sedimentary host rocks proximal to the deposits was considered a distinct possibility. In fact, over 140 years ago, Dantree (1866) proposed the idea that gold in the turbidite-hosted quartz reefs in the Victorian Goldfields was derived from organic matter originally precipitated in the marine sedimentary host rocks. Buryak (1964, 1982), Boyle (1979, 1986), Vilor (1983), and Kribek (1991) have proposed that release of gold from organic- and pyrite-rich shales during diagenesis and metamorphism was the most likely origin for the gold in many lode gold deposits hosted by metasedimentary rocks. More recently, Emsbo et al. (1999, 2003) showed that there is syn- and/or diagenetic gold in the Devonian Popovich Formation and proposed that it was a source for gold in Eocene deposits of the northern Carlin Trend. Our recent data, resulting from detailed studies on a number of deposits (Large et al., 2007, 2009; Meffre et al., 2008; Scott et al., 2008; Large et al., 2010) provides additional evidence to support these previous ideas.

Because sediment-hosted gold deposits are invariably enriched in arsenic and sulfur (typical As/Au ratios in ores are 50/1 to 500/1), we believe it is unrealistic to consider the source of gold in isolation from the source of arsenic and sulfur. Black shales are an ideal source rock for Au, As, and S, as all are enriched well above normal crustal levels. Data compiled by Crocket (1991) showed that carbonaceous black shales have a mean gold content of 6.7 ppb (based on 553 samples), compared with an average of 2.5 ppb Au for igneous rocks, 1.8 ppb bulk average for the upper crust (Taylor and McLennan, 1995), and around 1 ppb bulk average for the mantle (Crocket, 1991; Fig 3A). These data are consistent

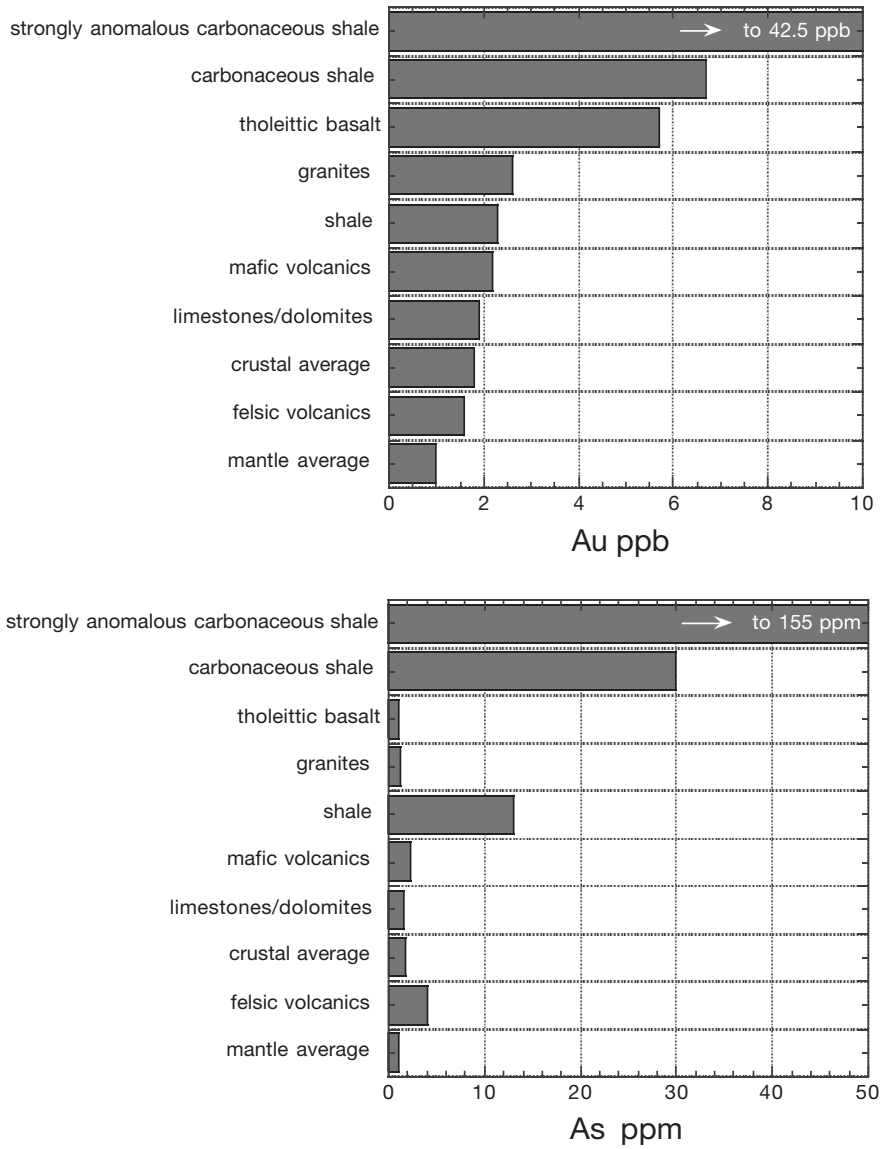

FIG. 3. Mean Au and As contents of crustal rocks compared with carbonaceous shales Data from Crocket (1991) and Ketris and Yudovitch (2009). Note this data indicates that carbonaceous shales are the most suitable source rock for both Au and As.

with a recent black shale trace element compilation by Ketris and Yudovitch (2009) who calculated a mean gold content of 7.0 ppb from over 9,000 analyses of black shales worldwide. They also report that the background population for gold in black shales is 3 to 20 ppb, with a strongly anomalous population varying from 35 to 50 ppb Au. This compares with data from the northern Carlin Trend where mean background gold in the Popovich and Roberts Mountain Formations is 28 ppb (Fig. 4A; Large, 2010).

Boyle and Jonasson (1973) suggested that shales have a mean As content of about 15 ppm, compared to all other crustal rocks, which contain 1 to 4 ppm. Quinby-Hunt et al. (1989), based on a worldwide dataset, suggested a mean As content of 29 ppm for carbonaceous black shales (Fig. 3B), which is about 16 times the normal crustal average. This is comparable with the recent compilation of Ketris and Yudovitch (2009) who reported a background mean of 30 ppm As, with a strongly anomalous range of 130 to 180 ppm As, from over 4,000 black shale analyses. Preliminary results from the Popovich and Roberts Mountain Formations in the northern Carlin Trend (Large et al., 2010; Fig. 4) suggest a generally high mean background As content of 36 ppm, away from mineralized zones, about 25 times the normal crustal average. The USGS standard black shale (SDO-1) has an As content of 68.5 ppm (Huyck, 1989). In contrast, mean As values for igneous rocks are 0.7 ppm for basalt and gabbro and 3 ppm As for granite and granodiorite (Reimann and de Caritat, 1998). However, the presence of As halos around some porphyry

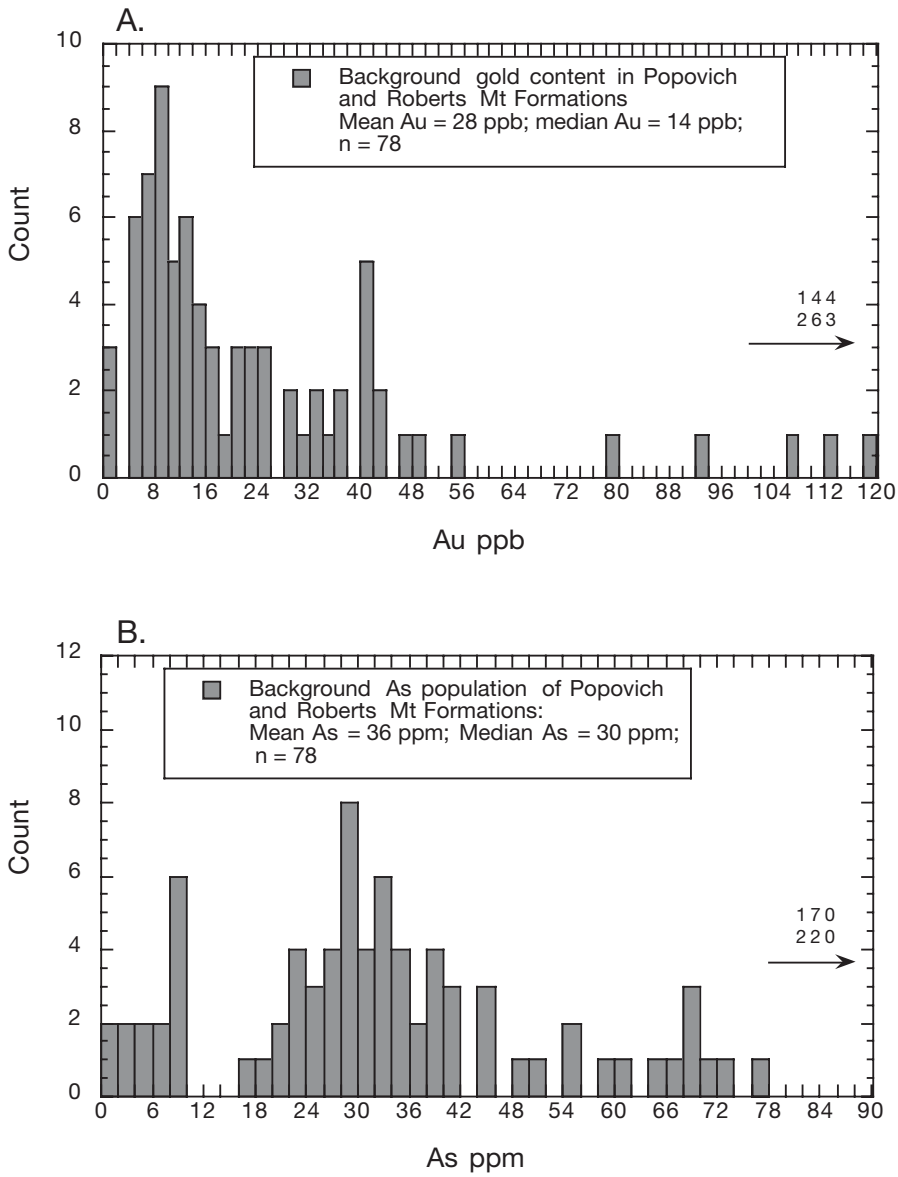

FIG. 4. A. Gold. B. Arsenic histograms of whole-rock values for unaltered carbonaceous and carbonate-rich sedimentary rocks from the Popovich and Roberts Mountain Formations, northern Carlin Trend. Data from Barrick drill holes CD12c, CD13c, and BSC168c to the west of Goldstrike. Each sample represents a composite from a 12-m section of drill core. Samples with evidence of alteration or hydrothermal mineralization have been eliminated from the data set.

copper deposits (Govett, 1983) suggests that some types of granite may be enriched in As above these mean levels. For example, a recent comprehensive study of the geochemistry of granites in the New England district of eastern Australia by Chappell (2010) has revealed an average As content of 5.5 ppm based on 1,261 samples. The S-type (reduced Ilmenite Series) granites in this database average 9 ppm As, and the I-type (oxidized magnetite series) granites average 5 ppm As.

Mean values of sulfur in crustal rocks vary from 700 to 950 ppm, with shales, black shales, and coals having the highest mean values of 1,100 and 20,000 ppm, respectively (Reimann and de Caritat, 1998). Igneous rocks generally have lower S contents than shales and vary from means of 100 (granite) to 900 ppm (gabbro and basalt).

In summary, carbonaceous black shales contain at least three times the crustal average for Au, 15 times the crustal average for As and 20 times the crustal average for S, and thus represent a suitable source rock for the sediment-hosted gold deposits considered here. Strongly anomalous black shales, as defined by Ketris and Yudovitch (2009), contain up to 28 times the crustal average for Au and up to 100 times the crustal average for As. No other crustal rocks have these attributes. Tholeiitic basalts and komatiites contain similar levels of Au (mean 5.7 ppm Au from 323 samples; Crockett, 1991), and have been considered as a potential gold source in greenstone terranes (Bavinton and Keays, 1978; Boyle, 1979; Keays 1987), however, they are depleted in As (mean 2 ppm; Boyle and Jonasson, 1973; Reiman and de Caritat, 1998) and are therefore a less likely source of a Au and As.

Why are black shales enriched in Au and As?

Several previous studies have shown that both organic matter and syngenetic and/or diagenetic pyrite in black shales can be enriched in gold and arsenic to significant levels above background. Anoshin et al. (1969) were the first to show that the gold content of modern sediments in the northern Atlantic Ocean, Mediterranean Sea, and the Black Sea was positively correlated with the organic carbon content of the sediments. For example, they demonstrated that in the Black Sea, the sediments with <1.5 wt percent $C_{organic}$ contained less than 2 ppb Au, whereas the organic-rich sediments with 2 to 4.5 wt percent $C_{organic}$ contained from 3 to 8 ppb Au (Anoshin et al., 1969; fig. 4). They concluded that the Au was extracted from seawater by biological activity and concentrated in the sedimented organic detritus. Vilor (1983) proposed that in anoxic deep-water depressions, like those in the Black Sea and the Sea of Okhosk, gold is deposited from seawater by flocculation and sedimentation of colloidal gold, which becomes adsorbed onto organic detritus, clay minerals, and iron sulfides in the black sea-floor muds. In a study of a turbidite sequence hosting gold mineralization in the Dongbeizhai and Jinya districts of southern China, Zhang et al. (1995) showed that gold was concentrated regionally with organic matter in the fine-grained black shale tops of turbidite cycles (Bouma sequence, CDE and DE units). Kerogens isolated from the black shale units contained 15 to 46 ppm Au. In the regional black shale host rocks (Khomolkho Formation) to the Sukhoi Log Au-As deposit in Siberia, Razvozzhaeva et al. (2002) reported the gold content of insoluble organic matter to be 1 to 2 ppm Au. Gold was found as organometallic complexes and nano-sized free gold particles in spirit-benzene bitumens and their asphaltene fraction.

Recent research on organic matter in the Popovich Formation in the northern Carlin Trend has also shown strongly elevated Au values (Emsbo and Koenig, 2007; Large et al., 2011; Scott et al., in prep.). The highest gold values (up to 100 ppm Au, Emsbo and Koenig, 2007) have been found in organic matter in the syngenetic Au horizon of the Upper Mud Member, in the Goldstrike mine area (Scott el al., 2011). In addition, our recent research has indicated that the fine-grained black mudstone tops to graded mass-flow units in the lower Roberts Mountains Formation, distal from the known gold deposits in the Carlin Trend, also contains organic matter with up to 4.5 ppm Au, 75,000 ppm As, 1800 ppm V, 780 ppm Sb, 690 ppm Mo, 425 ppm U, and 380 ppm Ni (Fig. 5, Table 2, Large et al., 2011).

Gold, arsenic, and other related trace elements may be introduced to the basin via rivers, by adsorption onto clay particles and organic detritus, which form part of the fluvial detrital input (Fig 6A). It is also likely that some gold is transported in rivers as finely dispersed microscopic grains (micronuggets) or in colloidal form (Reznik and Fedoronchuk, 2000). These authors propose that turbidity flows may transport the gold from its source, along paleovalleys and submarine canyons for more than 100 km, over the continental slope and into deep-water environments of the outer shelf.

The metals initially concentrate in black muds on the sea floor by desorption from clays, followed by reduction and adsorption, forming organometallic bonds with particular organic (humic and fulvic) compounds (e.g., Vilor, 1983; Kribek, 1991; Zhang et al., 1995; Nekrasov, 1996; Wood, 1996; Hu et al., 2000, Shpirt et al., 2007; Fig. 6A). Experimental studies by Zhang et al. (1997) indicate that bacteria may play a significant role in extraction of gold from seawater by adsorption onto,

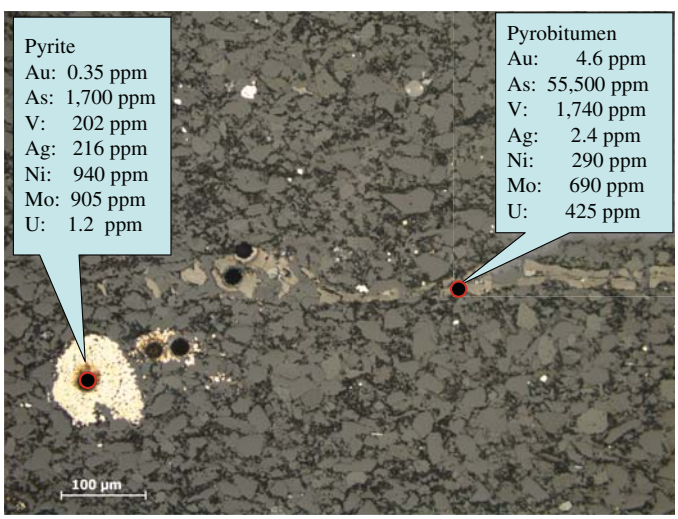

FIG. 5. Photomicrograph of a polished mount showing pyrobitumen after indigenous organic matter (light gray, bedding parallel) and diagenetic pyrite (white cluster of microcrystals) in a black mudstone from the lower part of the Roberts Mountain Formation, west of Goldstrike, Carlin district. Trace element analyses of pyrite and organic matter are by LA-ICP-MS (Table 3). The high levels of Ni, Mo, and Ag are typical for diagenetic pyrite from the Carlin district, and the high levels of V, As, U, and Mo are typical for organic matter (now pyrobitumen).

TABLE 2. Whole-Rock Analyses of Some Black and Gray Shales from Three Major Sediment-Hosted Au-As Provinces

	Pyritic black shale Khomolko Fm. Sukhoi Log 1/90.0	Black shale Khomolko Fm. Sukhoi Log 156a/17.5B	Gray calc-shale Khomolko Fm. Sukhoi Log 156a/17.5A	Black calc-mudstone UM Popovich Fm. Carlin GA54c/1460ft	Black calc-mudstone Roberts Mt Fm. Carlin CD13c/2524	Black shale Bendigonian Bendigo NBD 180w3/339.4	Gray shale Bendigonian Bendigo 172/537	Black shale SDO-1 Huyck (1989)	Black shale Average Ketris and Yudovitch -2005	Black shale Strongly anom. Ketris and Yudovitch -2005	Shale Average Wedepohl (1995)
SiO2	47.8	nd	nd	nd	nd	nd	nd	49.3	nd	nd	58.9
TiO2	0.34	0.87	0.15	0.13	0.19	0.38	0.45	0.71	0.3	0.6-0.8	0.78
Al2O3	9.3	16.1	4.6	3.0	4.6	14.6	16.5	12.3	nd	nd	16.7
Fe2O3	27.3	4.9	6.6	1.2	1.03	6.3	6.3	9.3	nd	nd	6.9
MgO	1.1	3.1	6.8	7.5	4.3	2.4	2.7	1.5	nd	nd	2.6
CaO	0.1	4.7	13.6	13.4	16.7	0.7	0.4	1.1	nd	nd	2.2
Na2O	0.17	0.51	0.36	0.05	0.01	0.53	0.77	0.4	nd	nd	1.6
K2O	3.1	3.9	1.1	1.1	2.8	3.6	4.0	3.4	nd	nd	3.6
P2O5	0.06	0.33	0.64	0.6	0.4	nd	0.11	0.11	0.14	0.30-0.38	0.16
TOC	nd	nd	nd	nd	0.74	0.84	0.05	9.9	nd	nd	0.2
Tot S	12.0	1.75	0.49	nd	0.73	nd	nd	5.4	nd	nd	0.2
Ag	1.4	<0.5	<0.5	3.9	0.4	0.2	0.1	0.13	1	4-5.5	0.07
As	**142**	**95**	**33**	**50**	**35**	**20**	**22**	**68.5**	**30**	**130-180**	**10**
Au ppb	**31**	**83**	**11**	**6**	**46**	**nd**	**nd**	**2.8**	**7**	**35-50**	**2.3***
Ba	620	700	180	590	160	760	810	397	500	1000-1400	580
Bi	<2	<2	<2	0.1	0.07	0.7	0.7	5	1.1	6-10	0.1
Co	13	20	6	3	3	16	18	47	19	40-50	19
Cr	50	115	28	260	21	80	77	66	96	220-280	90
Cu	127	30	22	108	11	84	37	60	70	230-310	45
Mn	100	402	1250	139	108	360	108	42	400	1200-1600	850
Mo	29.6	1.9	1	120	16	4.3	0.28	134	20	100-140	1
Ni	96	54	26	235	29	59	44	100	70	210-280	68
Pb	41	12	6	8	7	33	31	28	21	60-85	22
Rb	nd	147	38	45	60	nd	nd	126	74	170-200	140
Sb	5	4.2	2.1	30	10	2	1.4	4.5	5	17-23	1.5
Se	2.1	0.9	1.2	42	1.5	3	1	nd	8.7	50-70	0.5
Sn	nd	2.1	0.7	nd	1	4.8	6	29	3.9	15-20	6
Sr	40	375	1200	99	130	nd	nd	75	190	400-500	300
Te	<0.05	<0.05	<0.05	0.2	<0.05	<0.05	<0.05	nd	2	4-5	nd
Tl	0.98	0.5	0.1	2.5	1.04	1.2	1.3	8.3	2	15-25	0.68
U	11.3	4	1	20	5	6	4	49	8.5	40-55	3.7
V	108	109	33	2190	378	231	100	160	205	600-800	130
W	8	6	1	0.5	3.6	2.7	2.9	3.3	2.9	25-35	1.9
Zn	274	79	40	1900	446	368	114	64	130	470-640	95
Zr	196	nd	nd	nd	nd	nd	nd	165	120	260-330	160
V/(V+Ni)	0.53	0.67	0.56	0.90	0.93	0.80	0.69	0.62	0.75	0.74	0.66
V/Cr	2.2	0.9	1.2	8.4	18.0	2.9	1.3	2.4	2.1	2.8	1.4
Ni/Co	7.4	2.7	4.3	78.3	9.7	3.7	2.4	2.1	3.7	5.4	3.6
palaeo-redox#	Suboxic	Oxic	Oxic	Euxinic	Euxinic	Dysoxic	Oxic	Suboxic	Suboxic-anoxic	Anoxic	Oxic
V+Mo+Ni+Zn	507.6	243.9	100	4445	869	662.3	258.28	458	425	1625	294

No. interpreted paleo-redox is based on Ni/Co, V/Cr, V/(V+Ni), Mo, and U (Algeo and Maynard, 2004; Rimmer, 2004)

and combination with, amino acid secreted by the cell walls of the bacteria. There is also a possibility of the involvement of dissimilatory metal-reducing microorganisms (external electron acceptors) in the process (e.g., Kashefi et al., 2001). During diagenesis, dissolution of some organic matter and growth of diagenetic pyrite, related to bacterial reduction of seawater sulfate, leads to some transfer of the As and Au from the organic matter into the structure of the growing pyrite (e.g., Tribovillard et al., 2006; Fig. 6B). In the absence of reactive Fe or available H_2S to form pyrite, oxidation of organic matter

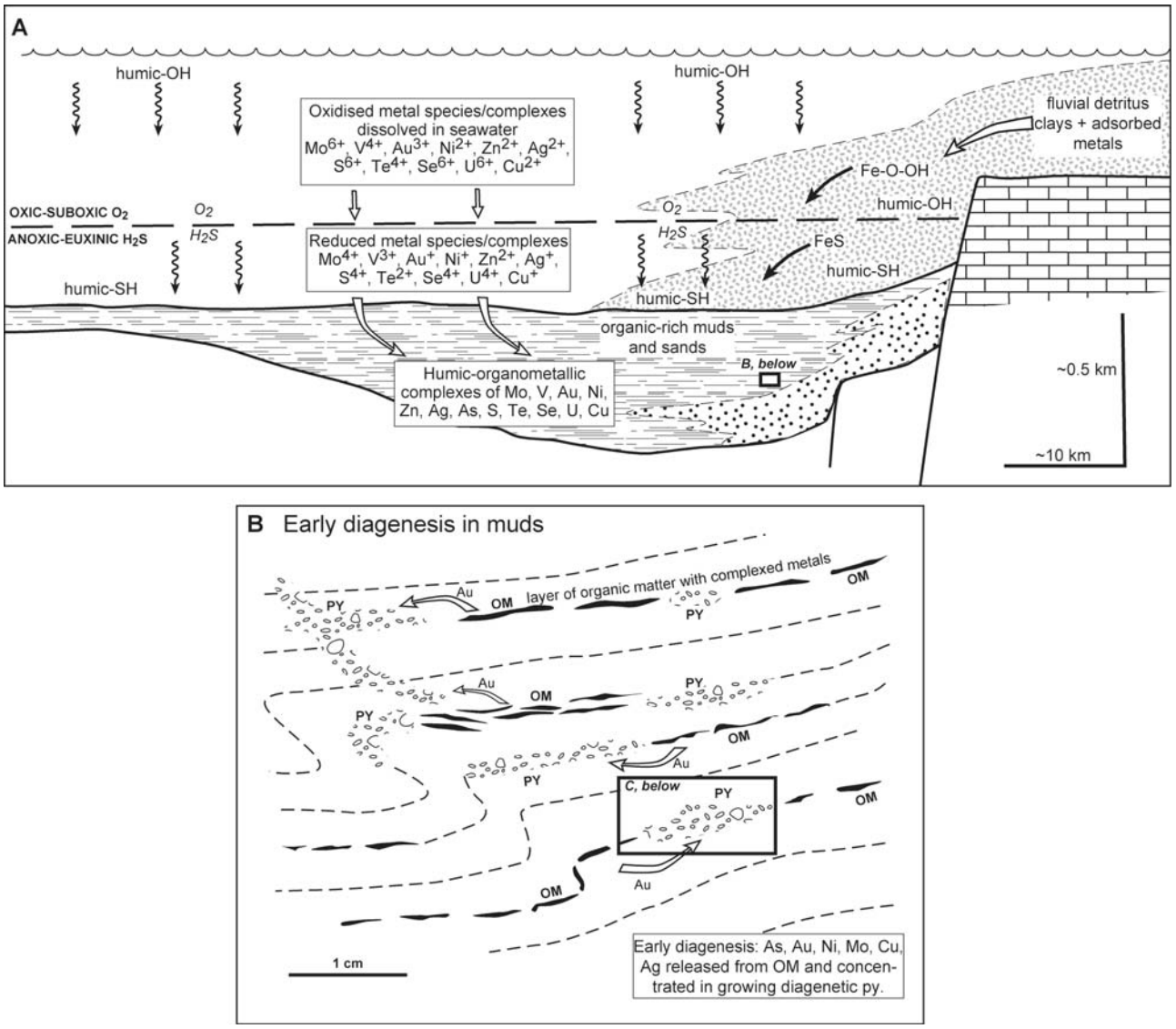

FIG. 6. Model for fixation and then release of gold from organic-rich pyritic muds in a continental basin margin setting. A. Gold and arsenic are introduced at the basin margins, adsorbed onto clays and iron oxyhydroxides that form part of the fluvial detrital input. Oxidized metal species and complexes are dissolved in the upper oxic to suboxic level of the stratified ocean. These become reduced in the lower anoxic to euxinic layers where they mix with pelagic organic matter (humic-SH species). In the organic-rich muds on the basin floor, gold, arsenic, and other metals form organometallic complexes with the humic material and become trapped in the muds. Model based on molybdenum cycle proposed by Helz et al. (1996). B. During early diagenesis organic matter dissolves and releases gold and arsenic (plus Mo, Ni, Pb, Ag, Cu, Zn, Te, Se), which pass into the structure of growing diagenetic pyrite (py1). The resultant arsenian py1 commonly contains from 0.5- to 5-ppm invisible gold. C. During late diagenesis and early metamorphism the sediment passes through the oil window resulting in migration of organics. Late diagenetic py2 overgrows may replace some of the py1, with consequent release of some gold to the ambient pore waters. During the late stages of deformation and metamorphism larger euhedral pyrites overgrow and partly replace the earlier gold-bearing pyrite. Gold dissolved in the replaced pyrite is released to form free gold grains in cracks or as a rim around the later pyrite. The organic matter remaining in the sediment is converted to pyrobitumen and ultimately graphite. In this process, further gold may be lost to migrating metamorphic fluids. At higher metamorphic grade (above middle greenschist facies) pyrite commonly converts to pyrrhotite (depending on the bulk-rock composition), with the loss of all remaining gold and arsenic. All these processes contribute to a gold enriched synmetamorphic fluid, which can redeposit the gold into favorable structural sites such as fold hinges or shear zones.

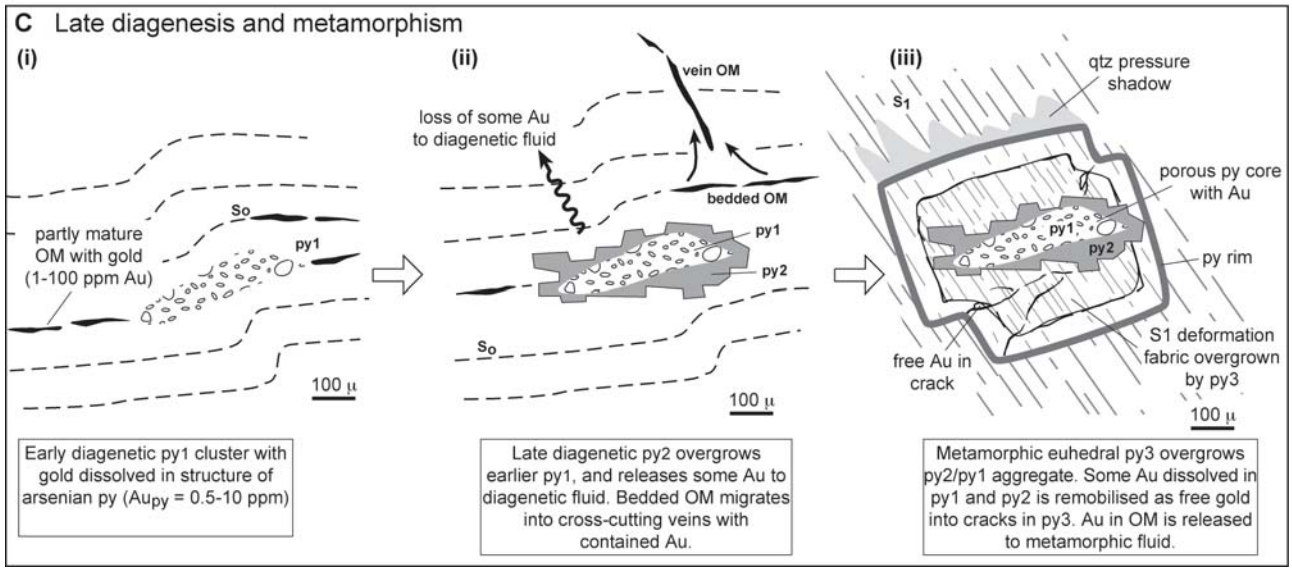

FIG. 6. *(Cont.)*

during diagenesis destroys organometallic complexes and releases the gold to form very small native gold particles (micro- and nanonuggets) in the black mudstones (e.g., Nifontov, 1961; Vilor, 1983). Based on studies of Russian black shales, Nekrasov (1996) estimated that most of the gold is present as micronuggets in carbonaceous matter (45–60%), with about 30 to 40 percent contained in syngenetic-diagenetic pyrite and from 10 to 15 percent adsorbed onto finely dispersed clays. The positive relationship between gold and organic carbon content in a group of unaltered black shales from the host-rock sequences at Bendigo and the northern Carlin Trend (Fig. 7) is supporting evidence for the key role of organic matter in concentrating gold within the shales. Other redox sensitive trace elements (V, Ni, As, Zn, Ag, and Cu) show a similar positive relationship with organic carbon in the carbonaceous sedimentary host rocks (Bull et al., in prep).

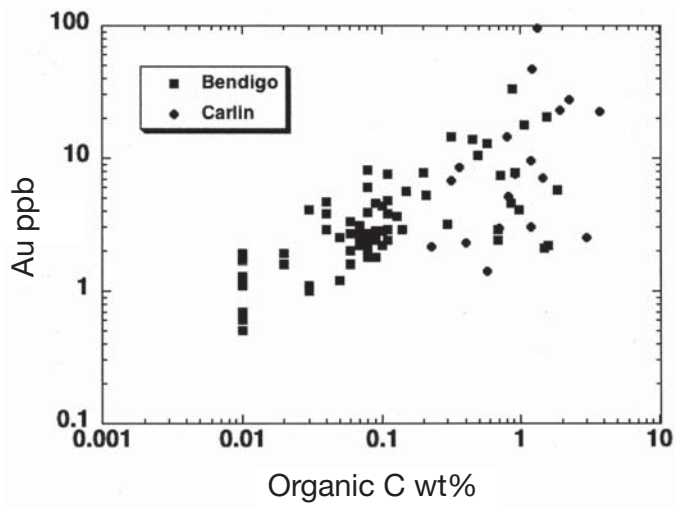

FIG. 7. Positive correlation between whole- rock gold and organic carbon content in a group of unaltered siltstones and carbonaceous shales from the Ordovician host sedimentary rocks at Bendigo and Devonian host sedimentary rocks (Upper Mud Member of the Popovich Formation) on the northern Carlin Trend. Data from Bull et al. (in prep.), Large et al. (2010, in press).

Emsbo (2000) has proposed an alternative model for the upper part of the Rodeo deposit in the northern Carlin Trend, whereby Au, As, and other metals are introduced by hot, H_2S-rich, basinal brines and fixed in organic carbon and pyrite on the floor of a submarine brine pool. Preliminary geochemical modeling by Hofstra and Emsbo (2004) has shown that while Au and As can be transported by such brines, many of the other introduced elements (e.g., V, Ni) in the syndiagenetic ore cannot, which led them to suggest that another transport medium (petroleum) may also be involved. Support for this suggestion is provided by the presence of native gold, vanadium mica, and other trace elements in veinlets of bitumen within and above the ore horizon (Emsbo et al., 1999, Emsbo and Koenig, 2005, 2007).

LA-ICP-MS analyses (Table A1 in electronic appendix; Fig. 8A) of diagenetic pyrite in the carbonaceous black shale host rocks lateral to a number of sediment-hosted gold deposits, including Sukhoi Log (Siberia), Bendigo (Victoria), and Rodeo (northern Carlin Trend), show Au contents of 0.001 to 142 ppm (mean 1.4 ppm Au) and As contents of 0.7 to 20,400 ppm (mean 2,550 ppm As) in the pyrite. These studies have shown that, distal to the ore deposits, the Au and As are not present in later hydrothermal overgrowths on the diagenetic pyrite (i.e., postdiagenesis), rather the metals are dissolved in the pyrite structure and concentrated in the cores of the diagenetic pyrite (i.e., syndiagenesis; Fig. 9; Large et al., 2009). In some very organic rich mudstones, with a low content of diagenetic pyrite, LA-ICP-MS analysis of the sedimentary rock matrix has revealed the presence of micronuggets of gold from 0.1 to 10 μm in the organic-clay matrix (Fig. 10).

Cabonaceous matter in black shales and gold ores

Carbonaceous sedimentary rocks associated with gold ore deposits have a wide range in total organic carbon (TOC). For example, the carbonaceous shales in the Khomolkho Formation, which hosts the Sukhoi Log gold deposit, are reported to

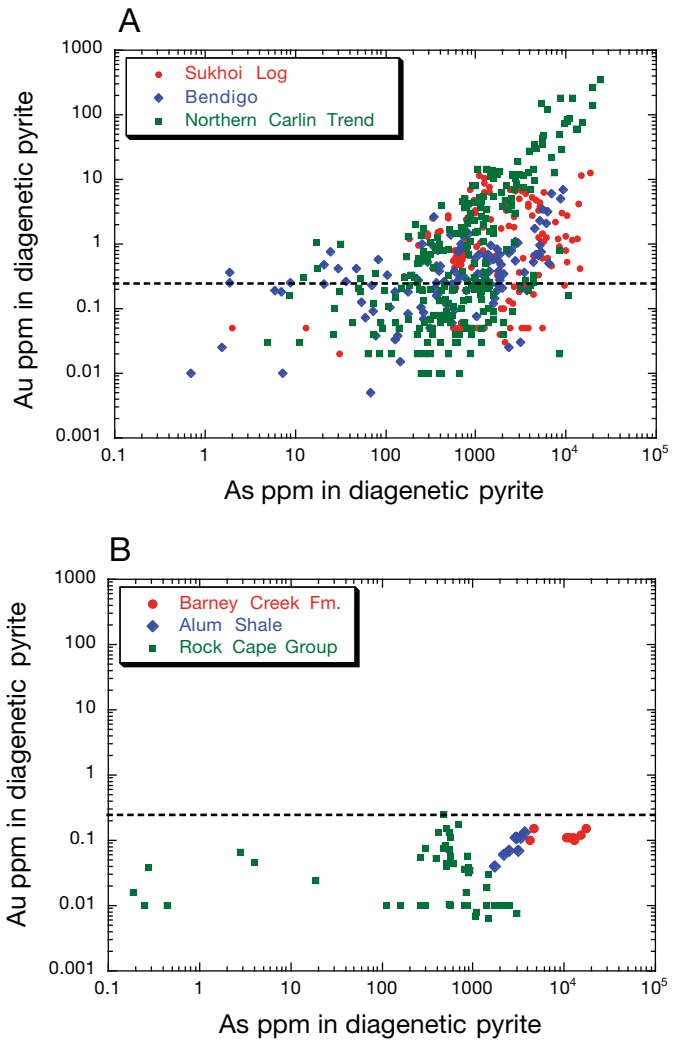

FIG. 8. Au-As plot for diagenetic pyrite. A. Productive carbonaceous shales. Data from Sukhoi Log (Large, et al., 2007), Bendigo (Thomas et al., 2010), and northern Carlin Trend (Large et al., in press). B. Unproductive carbonaceous shales (no known gold deposits). Data from this study.

have TOC values from 0.2 to 7 wt percent (Distler et al., 2004; Razvozzhaeva et al, 2008). There is no reported difference in TOC between the regional host rocks and the ore zones. In contrast the carbonaceous shales at Bendigo are generally less carbonaceous, with a range from 0.2 to 2.0 wt percent TOC (Thomas et al., 2011). In the northern Carlin Trend, the carbonaceous mudstone (Upper Mud unit of the Popvich Formation) that hosts the Rodeo deposit is variably carbonaceous from 0.2 to 15 wt percent TOC, with the highest TOC values close to the ore deposit. Shales in the Roberts Mountain Formation, which is the host to several other deposits in the Trend, vary from 0.3 to 3.7 wt percent TOC (Large et al., in press). In the higher metamorphic grade deposits at Sukhoi Log and Bendigo the organic matter has been converted to graphite, but in the low-grade Carlin-type deposits in Nevada, studies by Ilchik et al. (1986), Kettler et al. (1990), Leventhal and Hofstra (1990), and Hulen et al. (1994) suggest a range in maturity from "live oil' to overmature organic matter composed of cryptocrystalline graphite (Cline et al., 2005). In the Alligator Ridge district, the Yankee Carlin-type deposits contain "live oil" present as smears, vein and vug fillings in the basal Pilot Limestone (Hulen et al., 1994). GC-MS studies indicate that the most likely source of the oil is the overlying Pilot Shale, which has TOC values from 0.5 to 4 wt percent (Hulen et al., 1994).

Although most carbonaceous matter related to sediment-hosted gold deposits is considered to be indigenous to the local straigraphic units (e.g., Ilchik et al., 1986; Bao, 2001; Razvozzhaeva et al., 2008), some workers maintain that organic matter may be introduced from an external source during gold mineralization. For example, Pitcairn et al. (2006) used Fourier Transform IR analysis techniques to argue that most of the graphite in the Macraes gold ore, Otago district, was precipitated from the mineralizing hydrothermal fluids. Also in the Carlin district, Radtke (1985) suggested that the organic matter in the ores was introduced during the late stages of gold mineralization. More recently, Emsbo and Koenig (2007) have reported on the intimate association between gold and pyrobitumen in the Upper Mud member, Popovich Formation, Rodeo deposit, and concluded that gold was transported in indigenous petroleum, as organometallic compounds, during oil generation and migration in the Lower Mississippian.

Characteristic trace elements in black shales and Au-As ores

In addition to gold, trace elements that are commonly concentrated in orogenic gold deposits include (in approximate mean order of abundance): As, Cu, Zn, Cr, W, Ni, V, Pb, Sb, Bi, Te, and Mo (Boyle, 1986; Perring et al., 1991). This group is similar, but not identical, to trace elements present in Carlin-type deposits (in mean order of abundance): As, Zn, V, Sb, Cr, Sn, Ni, Cu, Te, Mo, Pb, Hg, W, and Tl (Bettles, 2002). Both groups have many overlapping elements with those concentrated in normal black shales (in order of abundance): V, Mo, Ni, As, Cr, Zn, Cu, U, Sn, Pb, Tl, Bi, Se, Sb, Te, and Hg (SDO-1 standard; Huyck, 1989; Table 2). Many of this element suite, in particular, Mo, V, U, Ni, Cr, As, and Cu, are redox sensitive trace elements that are indicative of reducing, anoxic to euxinic marine conditions, under which organic-rich black mudstones are deposited (e.g., Alegro and Maynard, 2004; Rimmer, 2004; Tribovillard et al., 2006). These trace elements can all form organometallic complexes with humic substances (Calvert and Pedersen, 1993; Wood, 1996; Tribovillard et al., 2006) and are readily reduced and trapped in sedimented organic matter on the sea floor (Fig 6A). Large (2010) proposed the term VAMSNAZ for black shales that are elevated in the redox sensitive elements: V, As, Mo, Se, Ni, Ag, and Zn, and where V score = V + Mo + Se + Ni + Zn >250 ppm. Of these elements, vanadium can be used as a proxy for the organic content of most marine sedimentary rocks (Quinby-Hunt and Wilde, 1993). Positive relationships between Au-V, and between Au and other redox-sensitive trace elements, which form organometallic complexes in whole-rock marine shale data, are a good indication that a process of gold concentration by complexation with organic matter or petroleum has taken place (Fig. 11).

During early diagenesis of the organic-rich muds, some trace elements, initially bonded with the organic matter (particularly As, Au, Mo, Se, Te, Ni, Pb, Cu, and Tl), are partitioned into, and concentrated within, the structure of diagenetic

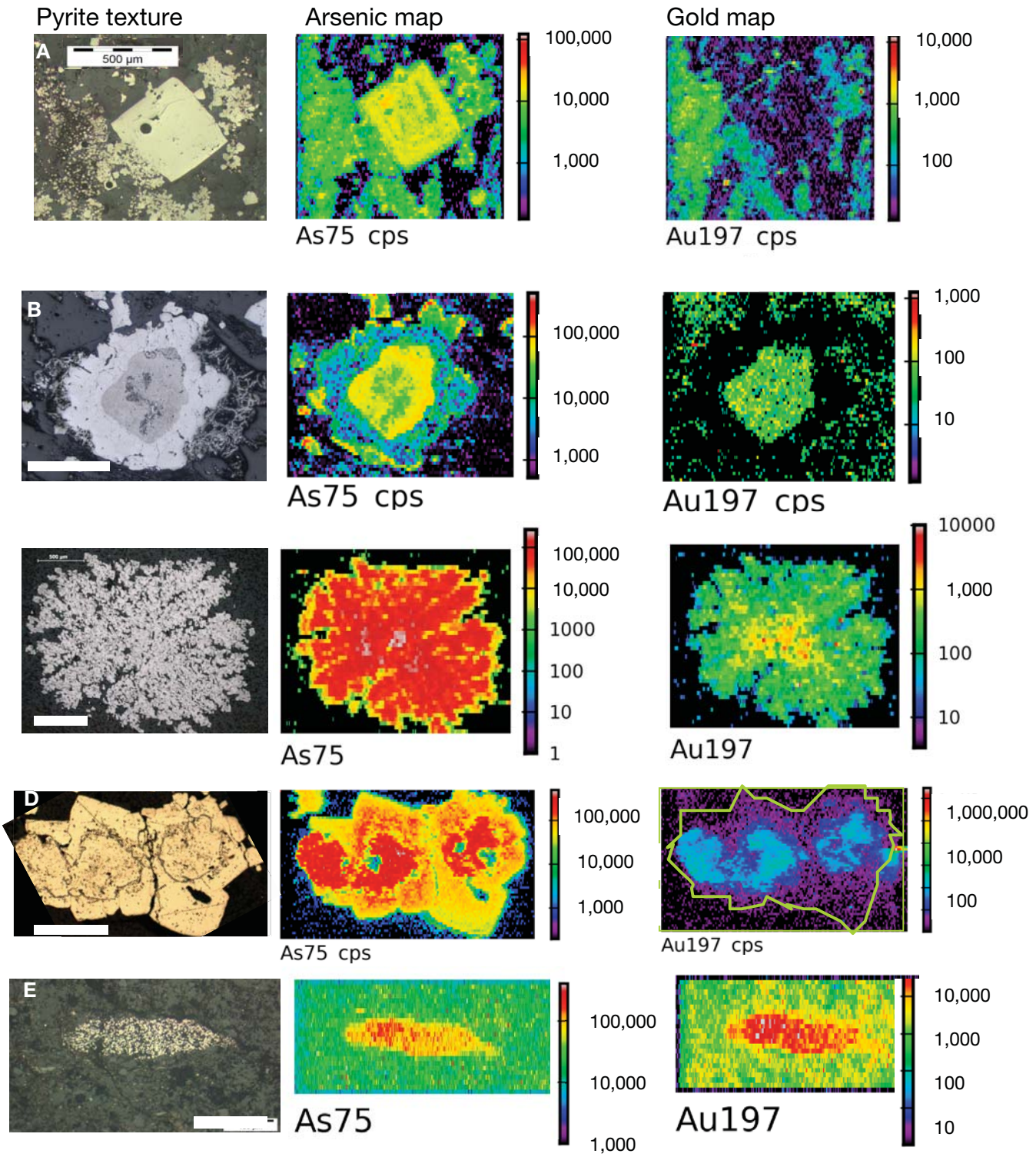

FIG. 9. Pyrite texture and related LA-ICPMS maps of Au and As in counts per second (cps) for typical diagenetic pyrites in carbonaceous shales from various gold districts. A. Sukhoi Log; fine-grained framboidal diagenetic pyrite on left-hand side is enriched in Au and As. Large euhedral metamorphic-hydrothermal pyrite is enriched in As but lacking in gold. Bar scale is 500 μm. B. Diagenetic pyrite nodule in carbonaceous shales, Kumtor deposit; fine-grained pyrite core is enriched in Au and As. Clear overgrowth of subhedral pyrite is devoid of Au. Bar scale is 1,000 μm. C. Starburst diagenetic pyrite in carbonaceous shale, Bendigo; highest gold occurs in center of pyrite aggregate, whereas As is elevated throughout. Bar scale is 500 μm. D. Zoned pyrite aggregate, carbonaceous shale, Spanish Mountain; gold is enriched in rounded diagenetic core of pyrite. Euhedral synmetamorphic outer zone of pyrite is devoid of gold. Bar scale is 500 μm. E. Diagenetic pyrite nodule composed of pyrite microcrystals enriched in gold and arsenic, Upper Mud Member, Popovich Formation, Rodeo mine, northern Carlin Trend. Bar scale is 100 μm.

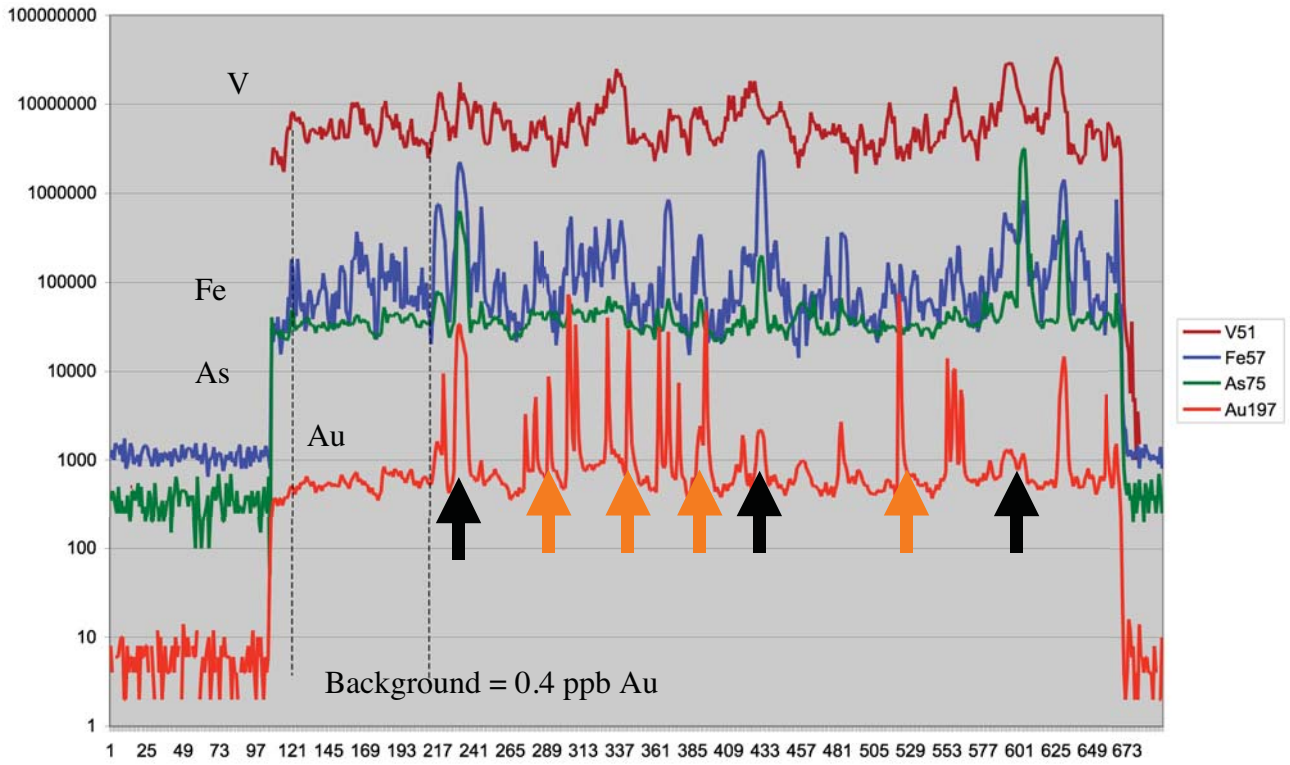

FIG. 10. LA-ICPMS trace across the matrix of an organic-rich mudstone from Carlin district, Upper Mud Member, Popovich Formation. Spikes in the gold trace are due to two sources: (1) invisible gold in arsenian pyrite (marked with black arrows and show coincident peaks in gold, arsenic, and iron), and (2) micronuggets of free gold (marked by the orange arrows; they show no coincident As and Fe peaks).

pyrite growing in the organic muds (e.g., Tribovillard et al., 2006; Fig. 6B). LA-ICP-MS analyses of fine-grained diagenetic pyrite, and pyrite after diagenetic marcasite, from several sediment- hosted gold deposits (Large et al., 2007, 2009; Table A1) show maximum trace element levels of 20,400 ppm As, 152 ppm Au, 2,700 ppm Mo, 4,500 ppm V, 3,400 ppm Zn, 12,600 ppm Cu, 4,200 ppm Se, 9,600 ppm Ni, 4,100 ppm Pb, 3,100 ppm Co, 1,200 ppm Sb, 670 ppm Ba, 440 ppm Tl, 340 ppm Ag, 275 ppm Bi, 68 ppm Te, 35 ppm U, and 27 ppm W. Although most of these trace elements are contained in the structure of the pyrite, others (e.g., V, Cr, Ba, U, and W) are present within silicate or oxide mineral inclusions in the pyrite. Our data suggest that gold levels in diagenetic pyrite in organic-rich shales in major gold provinces are typically in the range of 0.1 to 12 ppm Au (Table A1; Fig. 8B).

Importance of arsenic-rich shales

Fleet et al. (1993) and Reich et al. (2005) have shown that the arsenic content of hydrothermal pyrite controls its capacity to hold gold within the pyrite structure, with the more As rich pyrite commonly being the more Au rich for a given deposit. Large et al. (2009) have shown that the same relationship holds for diagenetic pyrite in black shale host rocks to the sediment-hosted gold deposits considered here (Figs. 8A, 12B). For example, As-poor diagenetic pyrite at Sukhoi Log contains 580 ppm As and 0.57 ppm Au, whereas As-rich diagenetic pyrite from the same deposit contains 3,600 ppm As and 6.18 ppm Au (Large et al., 2009; Table A1). Thus the capacity of black shale sequences to contain gold-enriched diagenetic pyrite is directly related to the arsenic content of the pyrite. Consequently, it is proposed that the best source rocks for sediment-hosted gold deposits of the type discussed here are arsenic and gold-rich shales. The fact that not all As-rich black shales contain anomalous gold, within the diagenetic pyrite, is the subject of ongoing research. Our data on pyrite from the carbonaceous Alum Shale in Sweden, for example, reveals up to 3,600 ppm As, 6,000 ppm Ni, and 600 ppm Mo, but only 0.04 to 0.13 ppm Au (Table A1; Fig. 8B).

Ultimate source of gold and arsenic in black shales

This model proposes that Au and As are concentrated in marine black shales (in both organic matter and diagenetic pyrite) by extraction from seawater and marine clay detritus during sedimentation and diagenesis. Some researchers (e.g., Titley, 1991; Coveney et al., 1992; Emsbo, 2000) have proposed that hydrothermal exhalation is required to enrich the basin waters with Au, As, and other metals in order to produce metal-rich black shales. Many studies have demonstrated that the gold content of seawater is not homogeneous, with reported variations from 0.001 to 0.50 ppb Au (Nekrasov, 1996). The highest gold concentrations have been found in seawater at continental margins and in the top layers of inland seas, such as the Black Sea (Henderson, 1985; Anoshin, 1997). Assuming that continental margin seawater contains on average 0.006 ppb Au, a concentration factor of about 10^3 is required if all the gold in average marine shales comes from

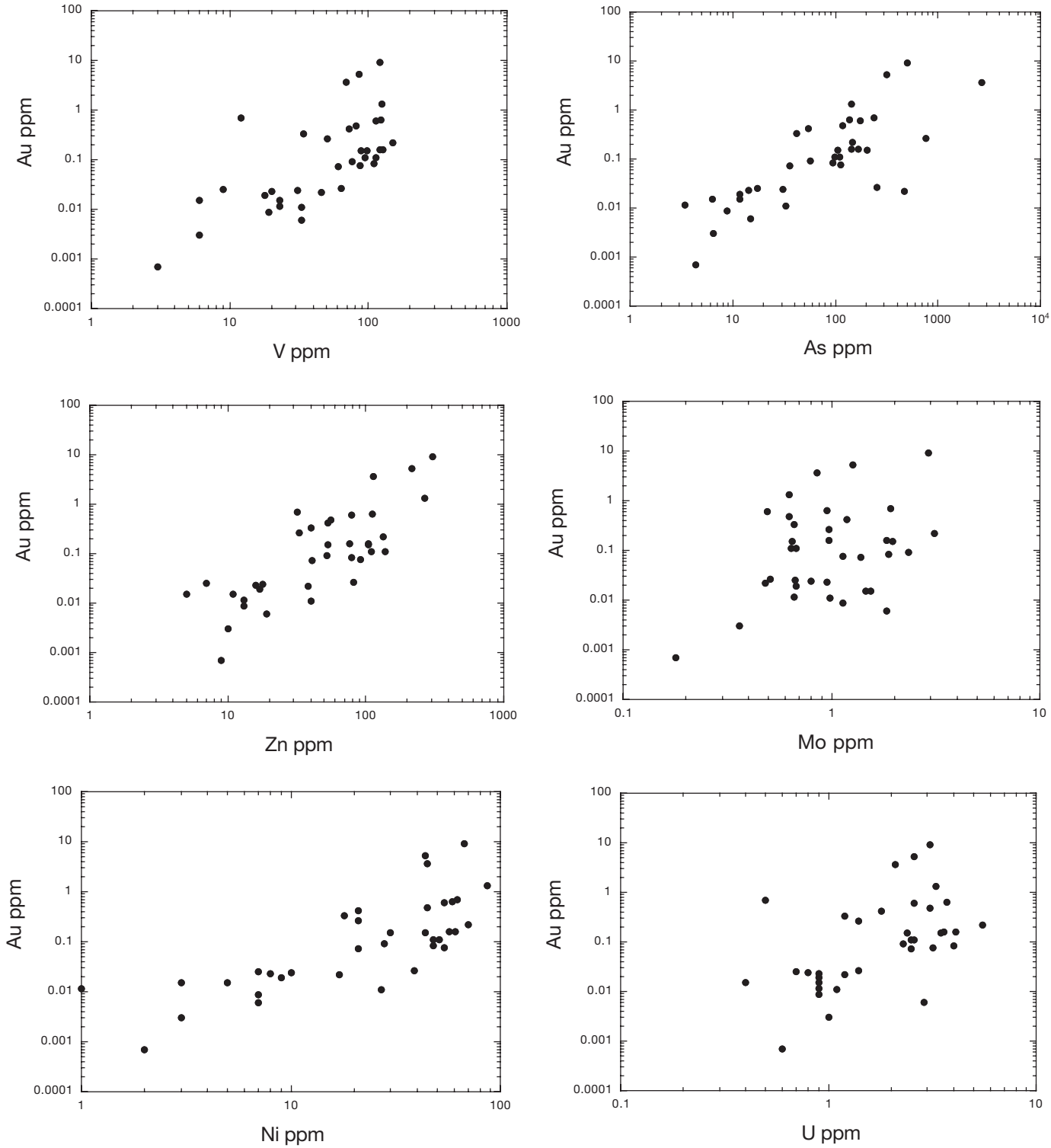

FIG. 11. Bivariate plots showing correlations between Au-V, Au-As, Au-Mo, Au-Zn, Au-Ni, and Au-U for carbonaceous sedimentary host rocks to the Sukhoi Log deposit. The linear trends on the log-log plots suggest a fundamental relationship of gold to V, As, Mo, Zn, Ni, and U.

seawater. This is less than the concentration factors required for Ni, Mo, Zn, and As in black shale and suggests that seawater is a viable source for background gold in black shales. Lehmann et al. (2007) maintained from their study of the Early Cambrian of southern China that concentration factors of ~10^7, with respect to present-day seawater, operated to produce highly metalliferous carbonaceous shales enriched in Mo, As, Ni, Zn, Cu, Se, Au, REEs, and PGEs. They concluded

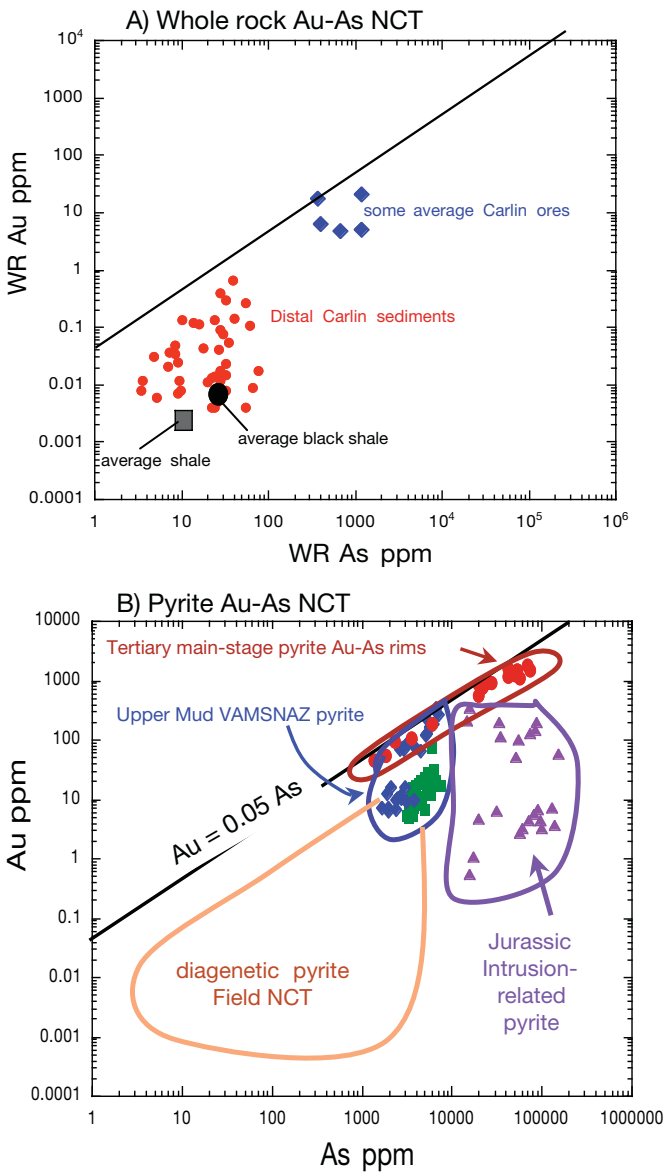

FIG. 12. Au-As relationships in sedimentary rocks, pyrite, and ores from northern Carlin Trend (NCT). A. Whole-rock calcareous black mudstones in the Popovich and Roberts Mountain Formations distal from ore (sediment data from Barrick drill hole CD 13c; ore data from Bettles, 2002). These data show that the Carlin sedimentary rocks commonly have higher values of Au compared with average shales and black shales. B. Pyrite types in the northern Carlin Trend. The Carlin main-stage Au-As-pyrite rims (red dots) plot parallel with and just below the gold saturation line for arsenian pyrite. The gold-rich diagenetic pyrite (blue diamonds and green squares) from the metalliferous horizon (MH) in the Upper Mud Member of the Popovich Formation commonly has an order of magnitude less gold than the main-stage rims. Most diagenetic pyrite plots well below the saturation line (see Fig. 8A). Pyrite associated with the Jurassic intrusions (purple triangles) is very As rich, with variable gold, and forms a separate field.

that metal extraction from seawater, in a sediment-starved euxinic basin, may produce concentrations up to 400 ppb Au and 10,000 ppm As in black shales.

Further research is required to resolve this issue of the relative importance of hydrothermal exhalation versus extraction from seawater onto organic matter during sedimentation.

Gold Upgrading During Late Diagenesis, Metamorphism, and Deformation

Syngenetic accumulation of gold-bearing organic matter and gold-bearing diagenetic pyrite in arsenic-rich black mudstones rarely produces significant economic deposits (i.e., large tonnages of ore above 1 ppm Au; Nekrasov, 1996), although the metalliferous horizon at Rodeo in the Carlin district may be an important exception (Emsbo et al., 1999; Scott et al., in prep.). However upgrading of low-grade syngenetic gold (from 0.02–2 ppm Au in the mudstones to 1–50 ppm Au in the ores) may occur during later diagenetic, metamorphic, tectonic, intrusive, or hydrothermal events (Kribek, 1991; Hutchinson, 1993; Mumin et al., 1994; Nekrasov, 1996).

With the onset of late diagenesis, the early forms of microcrystalline gold-bearing arsenian pyrite recrystallize to larger crystals (commonly <0.2 mm) of subhedral to euhedral pyrite, or in some cases pyrite nodules, developed parallel to bedding (Fig. 9; Large et al., 2007, 2009). Pyrite analyses indicate that some gold and other trace elements are released during this process forming a gold-bearing diagenetic fluid that may migrate and deposit free gold in late diagenetic structures. Nekrasov (1996) demonstrated that up to 20 percent of the gold adsorbed onto carbonaceous matter and the clay fraction of black shales can be extracted by weakly acidic, room temperature solutions after only 24 h of reaction. This suggests that diagenetic, meteoric, or metamorphic fluids in equilibrium with illite- or muscovite-bearing carbonaceous sedimentary rocks could mobilize gold from carbonaceous matter or clay minerals during fluid-flow events.

As the sedimentary rocks pass through the oil window, petroleum migrates along structures and may transport further gold (Hu et al., 2000; Williams-Jones and Migdisov, 2007). Such processes have been invoked in the Carlin district (Emsbo and Koenig, 2005, 2007; Large, 2010) and are proposed in the formation of the stratiform, black shale-hosted Nick (Ni-Zn-PGE-Au) deposit in the Yukon (Hulbert et al., 1992) and a number of black shale-hosted strata-bound gold deposits in the Mesoproterozoic, Cambrian, and Devonian strata of South China (Hu et al., 2000; Emsbo et al., 2005).

Further deformation and metamorphism (Fig. 6C) is accompanied by continued recrystallization and growth of pyrite. The syndeformation pyrite is commonly coarser grained (0.2–20 mm), with less sediment inclusions and a significantly lower trace element content (Chernoff and Barton, 2001; Large et al., 2007; Layton-Mathews et al., 2008), in particular Pb, Cu, Zn, Sb, V, Mo, Ag, Bi, Te, and Tl. Textural studies of deposits at greenschist facies of metamorphism suggest that the mobilized Pb, Cu, and Zn are reprecipitated as discrete microinclusions of galena, sphalerite, and chalcopyrite, which typically reside (along with pyrrhotite) in the cores of recrystallized pyrite aggregates (Large et al., 2007). If Te, Ag, and Bi are present in the diagenetic pyrite, then recrystallization leads to the formation of microinclusions of Pb-Bi + Ag + Au tellurides, as seen at Sukhoi Log and Spanish Mountain (Large et al., 2009). Molydenum tends to form molybdenite and V moves into the structure of white mica, replacing Al, a feature that is common in the Rodeo metalliferous horizon in the Carlin Trend. Not all trace elements are lost from pyrite in this process; As, Co, Ni, and Se are retained and may even become slightly enriched.

Invisible gold dissolved within diagenetic arsenian pyrite is released during pyrite recrystallization and becomes concentrated as (1) free gold grains within hydrothermal and/or metamorphic pyrite at the site of recrystallization; (2) invisible gold in hydrothermal arsenian pyrite rims on preexisting pyrite, within ores developed farther downstream from the zones of gold-arsenic release; or (3) free gold in quartz veins in structural zones, particularly, fold axes, faults, shears, and breccia zones. Later generations of metamorphic and /or hydrothermal pyrite commonly nucleate on early diagenetic pyrite, leading to zoned pyrite aggregates that display gold-enriched hydrothermal rims (e.g., Carlin-type deposits and Bendigo; Large et al., 2009; Thomas et al., 2010).

Conversion of diagenetic pyrite to pyrrhotite during metamorphism

Because pyrrhotite does not hold gold or arsenic in its structure, conversion of gold- bearing diagenetic pyrite to pyrrhotite during greenschist and amphibolite facies metamorphism is a very efficient method of releasing invisible gold and arsenic from pyrite into the metamorphic fluid, with ultimate precipitation of orogenic Au-As ores in a proximal or distal location depending on the physicochemical conditions (e.g., Buryak, 1982; Pitcairn et al., 2006; Large et al., 2007; Procenko, 2008; Tomkins, 2010). LA-ICP-MS data on diagenetic pyrite (mean 0.61 ppm Au, 1,325 ppm As) and metamorphic pyrrhotite (mean 0.04 ppm Au, 3.8 ppm As) in the sedimentary rocks at Bendigo (Thomas et al., 2010) indicate a 90 percent loss of Au and 98 percent loss of As associated with the pyrite to pyrrhotite conversion during metamorphism. The conversion is facilitated by organic carbon, available Fe (in silicates or carbonate), and water, as outlined in the following reactions (Ferry, 1981; Hoschck, 1984; Thomas et al., 2011):

$$2FeS_2 + 2H_2O + C \Leftrightarrow 2FeS + 2H_2S + CO_2, \quad (1)$$

and

$$FeS_2 + Fe^{2+} + 0.5\ C + H_2O \Leftrightarrow 2FeS + 2H^+ + 0.5CO_2. \quad (2)$$

Thus, reaction of meteoric or metamorphic water with organic-rich pyritic shales will promote the pyrite to pyrrhotite conversion, and consequent loss of arsenic, gold, and sulfur (eq 1) under lower to upper greenschist facies conditions (Fig. 13). Hofstra and Emsbo (2007) have emphasized the key role of carbon-bearing sediments in stabilizing H_2S and thus promoting gold transport as the soluble gold bisulfide complex within reduced sedimentary rock sequences, such as occur in the Great Basin, host to the Carlin-type deposits.

The contact metamorphic aureoles of any pluton are likely to go through the same pyrite to pyrrhotite conversion with consequent release of Au and As from preenriched black shale host rocks and drive meteoric fluid convection, resulting in an Au-As–rich hydrothermal fluid capable of forming Au ores in structural sites distal from the intrusion. Some intrusions may also add gold to the system via mixing of magmatic fluids with the meteoric fluids. If these processes are correct, then some intrusion-related gold deposits (Thompson et al., 1999; Goldfarb et al., 2005; Nutt and Hofstra, 2007) may have a significant contribution of Au and As from the sedimentary rocks into which the intrusions were emplaced. It is also conceivable that these processes may have been important in the Carlin-type gold districts where Jurassic, Cretaceous, and Tertiary intrusions into the Ordovician to Devonian arsenic-rich calcareous black mudstones are common (Sillitoe and Bonham, 1990; Seedorff, 1991; Henry and Boden, 1997; Hofstra et al., 1999; Ressel et al., 2000; Cline et al., 2005).

Scale of the gold-upgrading process

Our studies suggest that the scale of gold mobilization in carbonaceous shale sequences covers a spectrum from millimeter to centimeter scale during diagenetic pyrite recrystallization, to 100s of meters scale of gold reconcentration within the orebodies, to 10s of kilometers scale associated with regional mobilization of gold by fluid flow associated with metamorphism and/or deformation or associated with granite intrusion.

The millimeter to local orebody scale processes are well documented at Sukhoi Log (Large et al., 2007). The textural and compositional paragenetic evolution of pyrite at Sukhoi Log, from early synsedimentary py1 and syndiagenetic py2, followed by late diagenetic and/or early metamorphic synfolding py3, by syn- to late folding py4, and finally postpeak metamorphic py5, is paralleled by a systematic decline in invisible gold and trace element concentration of the pyrite. Although the gold dissolved in the structure of arsenian pyrite declines through the paragenesis, the amount of free gold present as inclusions in the pyrite increases. Thus free gold is only apparent as microscopic inclusions in the late diagenetic py3 to postpeak metamorphic py5. This suggests that diagenesis, deformation-metamorphism, and related pressure-solution processes have led to the liberation, remobilization, and redistribution of gold originally contained in the structure of early py1 and py2, to free gold which now occurs as inclusions and along fractures in the later syn- to postmetamorphic py3, py4, and py5 concentrated in the core of the Sukhoi Log anticline (Wood and Popov, 2006; Large et al., 2007). The process of gold upgrading which can be observed on the millimeter to centimeter scale by the pyrite paragenesis, and on the orebody scale by the gold grade distribution, is considered to have taken place across the full scale of the Sukhoi Log anticline, which measures 1 to 2 km across and 5 km in length.

The basin scale of gold mobilization and upgrading is more apparent at Bendigo. Here the source carbonaceous shales that host the quartz-bearing gold reefs extend within the Ordovician turbidite sequence up to a minimum of 3 km below the reefs and are thickened by structural repeats to around 7km (Willman, 2007; Willman et al., 2010; Thomas et al., 2011). Carbonaceous shales that exhibit the conversion of diagenetic pyrite to metamorphic pyrrhotite and represent the best source rocks for gold and arsenic are developed at 300 to 1,000 m below the productive reefs (Thomas et al., in press) but presumably extend to the base of the sedimentary pile, an additional 6 km. Thus the scale of fluid flow, gold remobalization, and concentration, associated with metamorphism of the carbonaceous turbidites, may span the full thickness of the sedimentary basin (Fig. 13).

Gold Depletion Zones

A consequence of gold mobilization from carbonaceous shales into superjacent ore deposits is that broad gold and

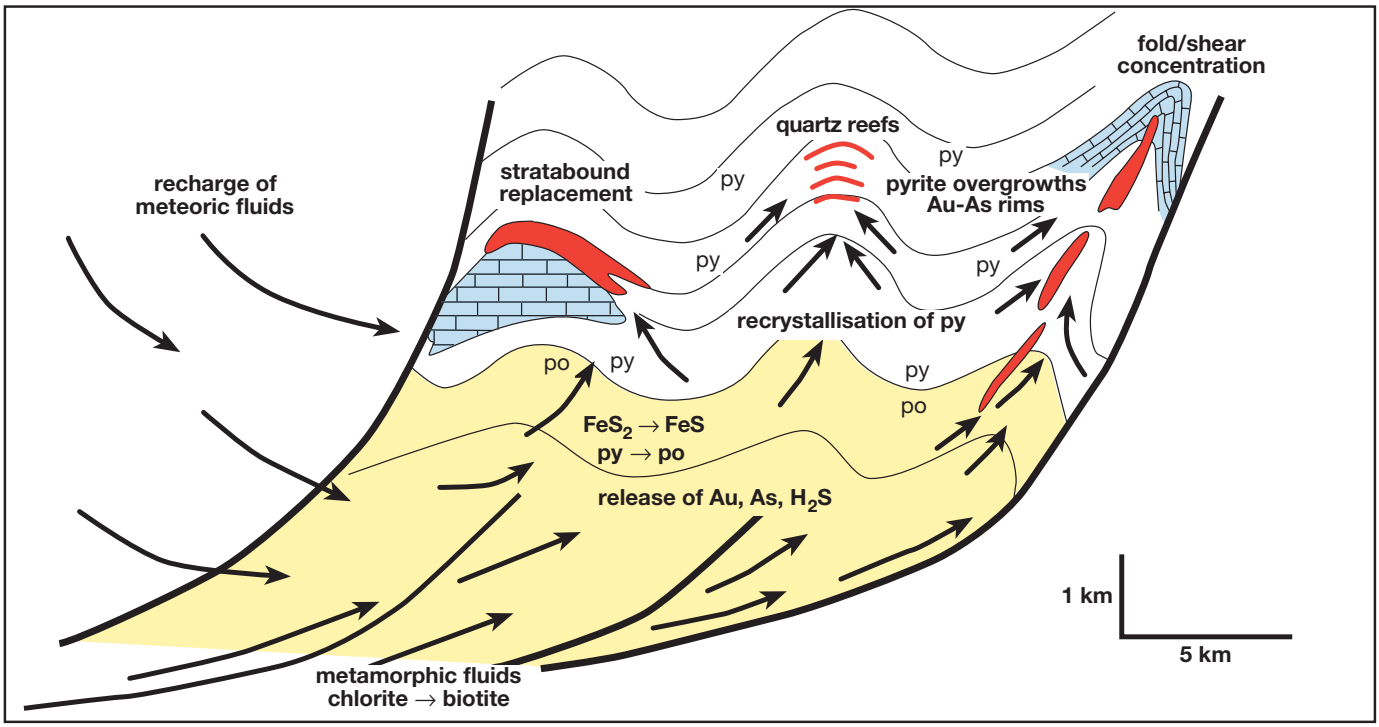

FIG. 13. Model showing potential meteoric and metamorphic fluid pathways; gold, arsenic, and sulfur is released from the carbonaceous sediments by conversion of sedimentary pyrite to pyrrhotite deeper in the basin (mid to upper greenschist facies). Gold and arsenic are deposited in the upper stratigraphy, associated with focusing of fluids along faults and into anticlinal zones or shears, and along favorable rock contacts. Pyrite overgrowth textures, and Au-As-rich rims, are common in the zones of gold concentration.

arsenic depletion zones should be present surrounding or below the ore deposits. However, metal depletion is a difficult process to measure and convincingly demonstrate because there is rarely sufficient drilling outside the mineralized zone to provide samples of the sedimentary rocks in the potential depletion zone and beyond in the barren sedimentary succession. Not withstanding these problems, a recent study by Goldberg et al. (2007), which involved sampling sedimentary rocks across the Victorian goldfields, has proposed that broad gold depletion halos surround the major ore deposits at Bendigo and Castlemaine. Regional analyses of sediments throughout the goldfields show a gold concentration halo averaging 14 ppb Au immediately surrounding the deposits, followed by an outer depletion halo of <0.5 ppb Au covering an area of more than 900 km^2. The background gold content of the regional sedimentary rocks was reported to be between 0.7 and 4.7 ppb Au (Goldberg et al., 2007). Also in the Otago orogenic gold province in New Zealand, Pitcairn et al. (2006) have reported extensive zones of gold, arsenic, and trace element depletion in the mid to high metamorphic grade metasedimentary rocks compared with the low-grade facies. They demonstrated that the depleted suite of elements (Au, Ag, As, Sb, Hg, Mo, and W) are the same as those enriched in the gold deposits of the province.

Sulfidation and the Source of Sulfur

Most researchers consider that sulfidation of iron-bearing minerals (magnetite, Fe silicates, or Fe carbonate) in the host rock is the cause of pyritization and gold deposition in orogenic and Carlin-type deposits (Phillips and Groves, 1983; Hofstra et al., 1991; Hofstra and Cline, 2000; Emsbo et al., 2003; Kesler et al., 2003; Cline et al., 2005; Goldfarb et al., 2005).

$$\underset{\text{Fe mineral}}{Fe^{2+}} + \underset{\text{ore fluid}}{2Au(HS)_2^-} + 2H_2 \Leftrightarrow \underset{\text{pyrite and gold deposition in rock}}{FeS_2 + Au^0 + 2H_2S}. \quad (3)$$

This process assumes that sulfur is transported in the ore fluid along with gold, in a soluble bisulfide complex. However, recent work (Chang et al., 2008) has shown a parallel relationship between the S isotope composition of pyrite in many sediment-hosted orogenic gold deposits, and the S isotope composition of coeval seawater sulfate through geologic time (Fig. 14). This is evidence that the reduced sulfur in these deposits may originally have been derived from seawater, a proposal previously suggested by Goldfarb et al. (1997) for a group of orogenic gold deposits in Alaska. Later introduction of gold and sulfur together, from an external fluid unrelated to seawater, is contrary to the sulfur isotope pattern in these deposits. If the sulfur source for sediment-hosted orogenic gold deposits was either magmatic or deep metamorphic, then there should be no relationship to the seawater sulfate curve through time (Fig 14).

Tectonic Environments and Favorable Basins

Favorable basins

As pointed out by Hofstra and Emsbo (2007), favorable sedimentary basins for gold ore deposits contain thick, reduced

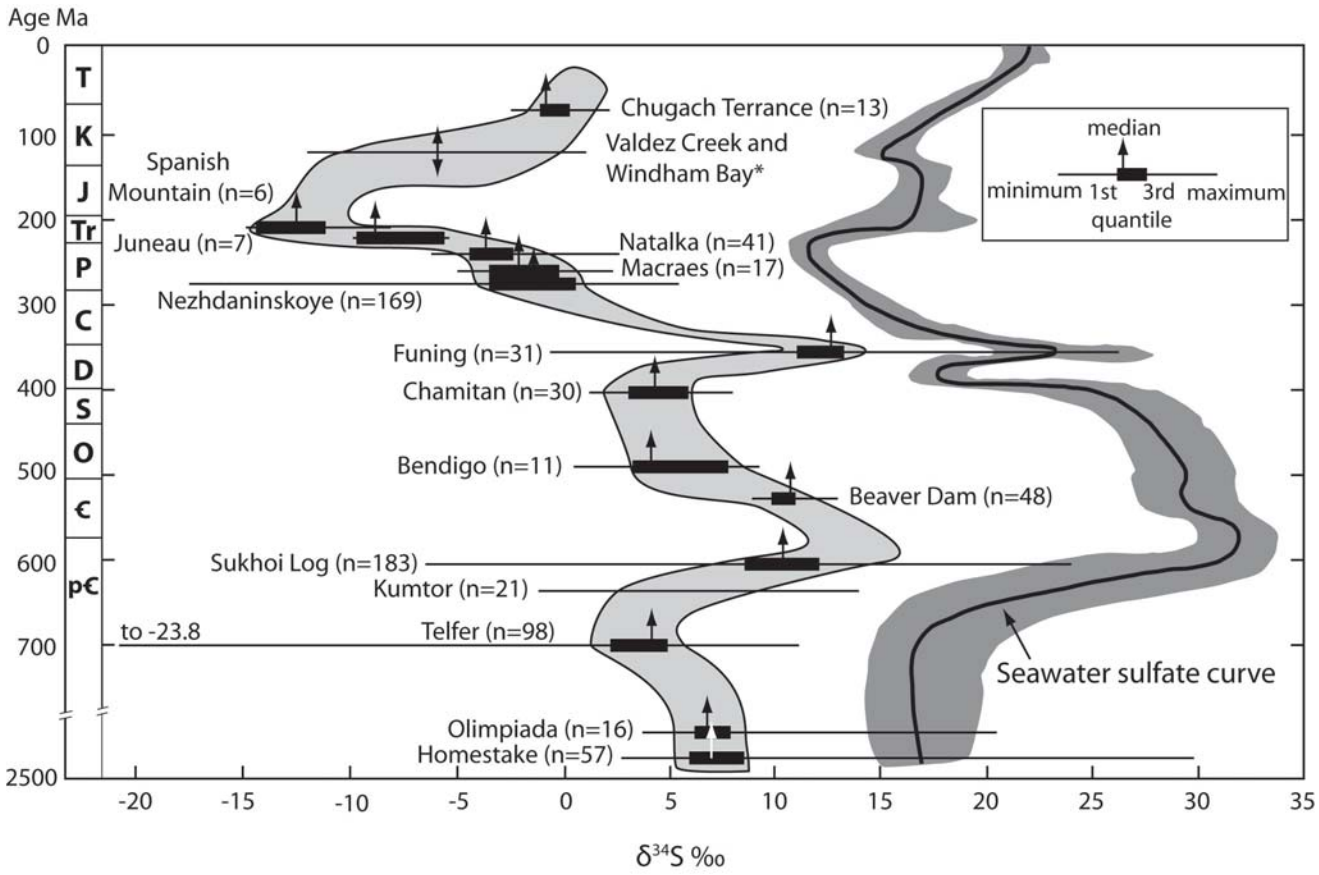

FIG. 14. Plot of sulfur isotope composition of pyrite vs. age of sedimentary host rocks for some sediment-hosted gold deposits, showing a general parallelism between $\delta^{34}S$ of pyrite in the deposits with the sulfate $\delta^{34}S$ value of seawater through time (from Chang et al., 2008). This suggests that seawater is the ultimate source of S in the ore deposits.

organic-rich sedimentary sequences in passive margin settings. We contend that interbedding of black mudstone and coarser clastic beds (sandstone, siltstone, graywacke) is important, because the mudstones are the initial source for gold trapped in organics, whereas the clastic rocks provide permeable zones facilitating gold-bearing fluid release during late diagenesis and metamorphism. Thick turbiditic successions record the former presence of an extensive deep-water body—either a large lake or the floor of a marine basin. As far as can be ascertained from the literature, all of the major gold-bearing turbiditic successions record marine sedimentation. However the precise setting within the marine realm can vary, as exemplified by the Carlin and central Victorian gold provinces, which can be considered as end members.

The host rocks for the central Victorian gold province, the Castlemaine Group, are a thick (~3 km), broadly upward-fining succession of Lower to Middle Ordovician siliciclastic turbidites and black shales (VandenBerg et al., 2000). Although they are now part of an easterly verging fold and thrust stack, making paleogeographic reconstruction difficult, there is no evidence of shallow-water conditions and/or a basin margin setting (i.e., intercalated shallower water facies, sedimentary structures indicative of reworking of the substrate, slope deposits, etc.). As a result the succession is interpreted to have been deposited seaward of the continental slope and rise on the deep ocean floor (Cas et al., 1988). With the exception of the basal part of the Castlemaine Group, which consists of sheetlike sandstone bodies, the turbiditic sandstones occur in overlapping lenticular bodies that have been interpreted in terms of submarine fan facies models (VandenBerg et al., 2000). Their siliciclastic provenance reflects derivation in response to ~15 km of uplift in the contemporaneous Delamerian fold belt to the west (Turner et al., 1996). Intercalated intervals dominated by black shales and cherts are common to Ordovician successions worldwide and have been interpreted to reflect global ocean anoxic events (Arthur and Sageman, 1994).

The host rocks for the Carlin gold province record a very different deep marine setting. They were deposited in slope and basin floor subenvironments immediately outboard of a major carbonate reef system that existed on the protowestern continental margin to the northern American continent from the Early Ordovician to the Late Devonian (e.g., Cook, 2005). In the northern Carlin Trend the host succession comprises a 4,500-m-thick package of black shales with varying proportions of intercalated turbidites. These slope and basin floor deposits interfinger with the coexisting carbonate reef system, locally termed the Bootstrap Limestone, and as a result, the succession has a distinctly calcareous provenance; the

mudstones are calcareous and the sandstones are often dominated by clastic carbonate grains such as ooids.

Although the depositional system was clearly a stable passive margin over a long time period, there is evidence that the host rocks to the bulk of the Carlin ores, the Lower to Middle Devonian Popovich Formation, was deposited during a period of synsedimentary tectonism and subbasin formation (Matti and McKee, 1977; Emsbo et al., 1999; Emsbo, 2005). The restricted subbasins were sites of deposition of highly organic mudstones.

The Sukhoi Log deposit in Siberia is situated in a similar continental margin basin setting to Carlin. The Neoproterozoic host sedimentary rocks of the Patom Group contain shelf, slope, and basinal facies in the Bodaibo trough sequence surrounding the deposit (Kazakevich, 1971; Wood and Popov, 2006).

Relationship of gold deposits to ocean anoxic events

Ocean anoxic events occur when Earth's oceans become depleted in oxygen to levels at, or very close to, zero (Strauss, 2006). These correspond to periods of widespread black shale deposition at continental margins and in restricted basins, with corresponding enrichment in organic matter, sedimentary pyrite, and redox-sensitive trace elements (Mo, V, U, Ni, Cu, Zn, Pb). Titley (1991) was the first to point out the coincidence of sediment-hosted gold deposits with strata deposited during episodes of ocean anoxia. He had no explanation for the coincidence but suggested that reduced oceans may have been favorable for the enhancement of gold in certain strata. The model proposed here provides an explanation for the coincidence, because Au and As become enriched in organic matter and diagenetic pyrite in the reduced continental margin sediments, along with other redox sensitive elements, during the ocean anoxic events (Fig. 6A). This concept may be tested by comparing periods of ocean anoxic events through time, with the age of host rocks for Au-As deposits (Fig. 15). Based on the ocean anoxic events defined by Strauss (2006; Fig. 15), we agree with Titley's original observation, that the correspondence of ocean anoxic events to sediment-hosted Au-As deposits is likely to be more than coincidence, taking into account the expected age uncertainties for the host black shale sequences.

Capacity of basins to produce gold deposits

Boyle (1979) was the first to introduce the concept of the capacity of various rock types to supply gold to economic deposits. Hofstra and Cline (2000) demonstrated that if 1 ppb Au was scavenged from sedimentary rocks in the source area to produce the deposits in the Carlin Trend, and the fluids interacted with only 10 percent of the source rocks, then a source region of 10 × 20 × 50 km would be required. They concluded that either the hydrothermal processes were crustal scale or the source rocks were gold enriched. In the two-stage model present here, the source rocks are gold enriched by the sedimentary-diagenetic processes involved in stage 1 (Fig. 16A). In the sedimentary source rock model, the capacity of metamorphosed sedimentary basins to produce gold-arsenic deposits depends principally on the primary (syngenetic and/or diagenetic) content of gold in the sediments that make up the basin. This is outlined in Table 3 below, where it is assumed that 80 percent of the primary sedimentary gold has contributed to the gold resource of structurally controlled and upgraded gold deposits.

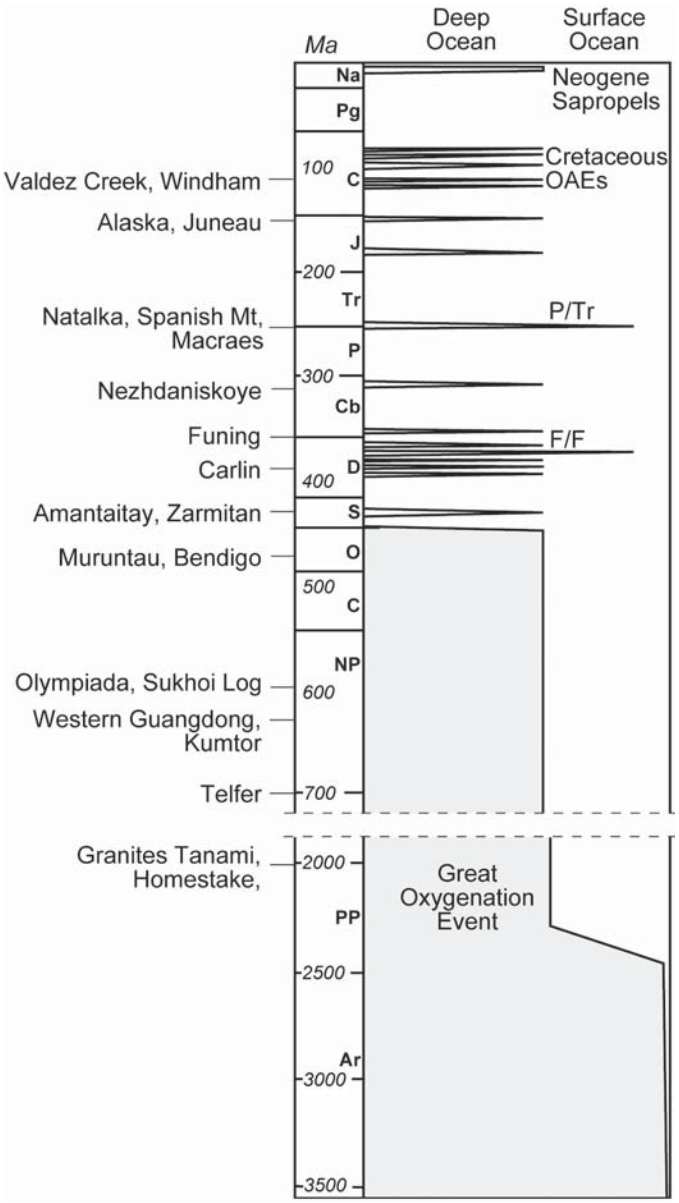

FIG. 15. Relationship between ocean anoxic events (OAE) and the ages of host rocks to some major black shale-hosted gold deposits (OAE from Strauss, 2006). Major sediment-hosted gold deposits are listed on the left-hand side, in order of the main age of their sedimentary host rocks. The spikes on the age chart correspond to periods of oceanic anoxia and widespread black shale sedimentation at continental margins.

This analysis indicates that sedimentary basins composed principally of average carbonaceous black shales (mean 6.7 ppb Au) have a capacity to produce orogenic gold deposits with a maximum resource of 0.52 million ounces (Moz) Au/km^3 of basin sediments. Strongly anomalous organic-rich basins as defined by Ketris and Yudovitch (2009), which may average up to 43 ppb primary gold in the shales, have the capacity to develop one or more deposits with a total resource of 3.36 Moz Au/km^3 of basin sedimentary source rock.

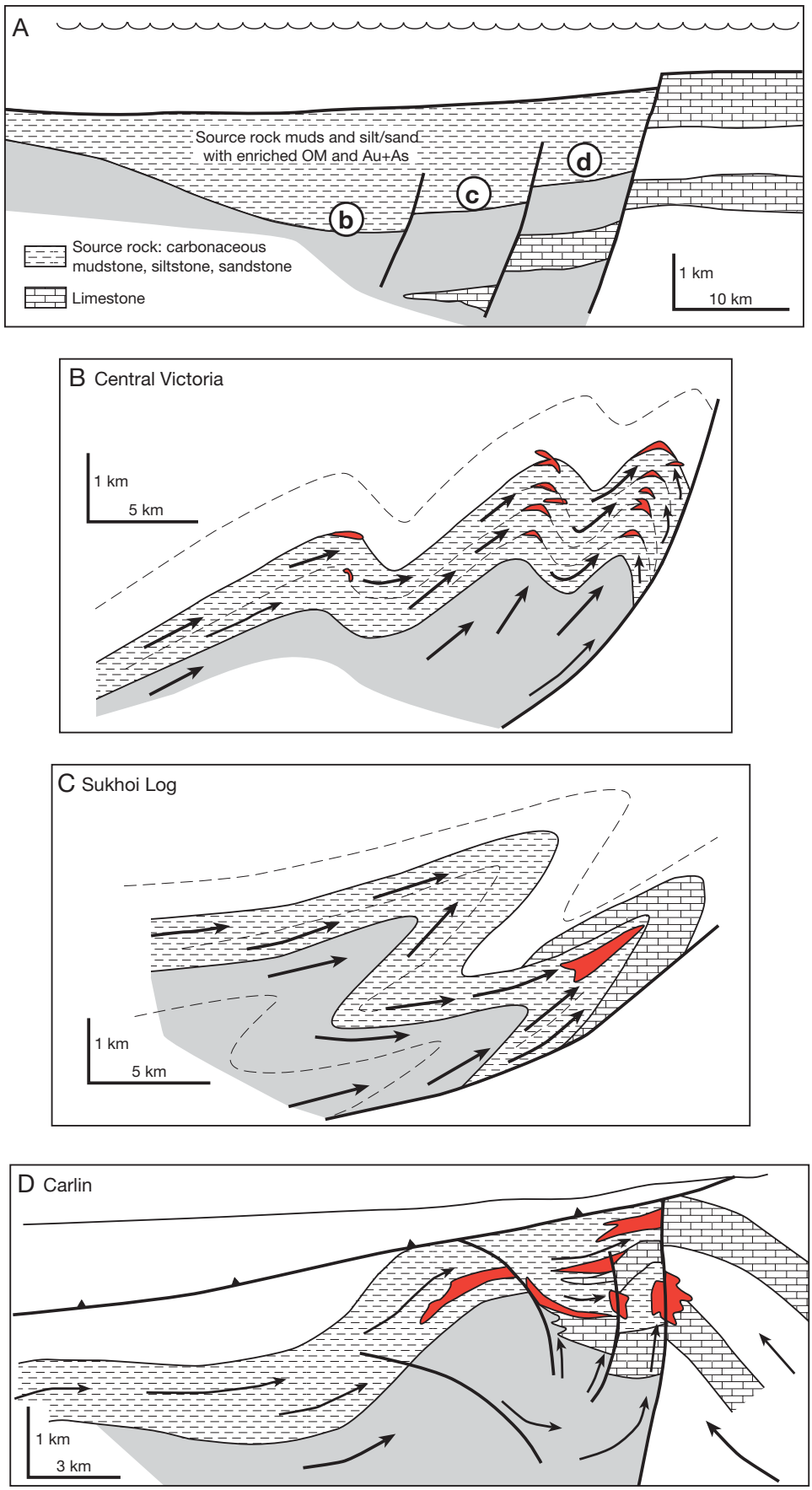

FIG. 16. Proposed model for formation of continental margin, sediment-hosted gold deposits. The sediment package in each diagram is regionally enriched in organic matter and Au-As during sedimentation. The lower stratigraphy may also be carbonaceous and Au-As enriched. Three examples from basinal settings increasingly proximal to the continental margin (B to D) are used to highlight the processes of gold concentration during deformation. A. Sedimentation of Au-As–bearing source rocks in a continental margin setting. Au and As occur trapped in organic matter and diagenetic pyrite within the carbonaceous sediments. B. The Victorian deposits formed in a sandstone-dominated turbidite sequence in a distal basin position (position b) with respect to the continental margin. Compressional tectonics associated with closure of the basin drove H_2S-bearing metamorphic fluids through the sandstones toward the elevated basin margin. Gold and arsenic were stripped from the interbedded organic-bearing shales associated with conversion of pyrite to pyrrhotite along the fluid pathways. Au and As are concentrated, along with silica, in quartz reefs at anticlinal crests (Fig. 1C, D). C. Sukhoi Log forms in a carbonaceous siltstone-mudstone–carbonate sequence (Khomolkho Formation) of slope facies closer to the interpreted continental margin. During compression, fluids move through the gold-arsenic–enriched carbonaceous siltstones to deposit Au-As and disseminated pyrite in an anticlinal core zone above a regional thrust. D. The northern Carlin Trend is positioned proximal to the carbonate-rich continental margin (positioned in A). Gold and arsenic, enriched during sedimentation, in the carbonaceous Roberts Mountain, Popovich and Rodeo Creek Formations, were stripped by meteoric fluids as they moved laterally through these formations toward the continental margin reefs, under the influence of compression, followed by extension, and/or Tertiary intrusions. Gold and arsenic are deposited in microrims on previous diagenetic pyrite, with concentration in structural sites or strata-bound zones.

TABLE 3. Capacity of Various Sedimentary Rock Types in a Basin to Act as Gold Source Rocks

Average gold content of sediments in basin (ppb)	Dominant sediment type in basin	Gold ore resource capacity per cubic kilometer of basin sediments (Moz)
1.9	Limestones and dolomites	0.15
2.5	Average shale	0.2
6.7	Carbonaceous black shales	0.52
12	Anomalous black shale	0.96
43	Strongly anomalous black shale	3.36

If our model is correct, this approach can provide an evaluation tool for gold exploration and mine development, similar to that developed to evaluate the oil potential of sedimentary basins by the petroleum industry. For example, available drill hole geochemical data west of Goldstrike (Barrick drill holes CD12c, CD13c, and GA 54c; Large et al., in press) indicates that the unaltered sedimentary rocks of the Popovich and Roberts Mountains Formations average 28 ppb Au and 36 ppm As (Fig. 4) away from zones of mineralization. If these values are representative of the background sediments (source rocks), then a corridor 15 km long, 2 km wide, and 2 km thickness (similar dimensions to the northern Carlin Trend) would have the capacity to yield a resource of up to 65 Moz of gold, assuming that the host stratigraphy originally contained 28 ppb Au, and 40 percent of the gold was released and concentrated to form the deposits. This compares favorably with the over 60-Moz production and reserve estimate for the northern Carlin Trend (Jory, 2002).

Do All Carbonaceous Shales Contain Syngenetic Gold?

The common occurrence of early gold concentrated in diagenetic pyrite within carbonaceous shales that host orogenic and Carlin-type deposits begs the question whether all carbonaceous shales contain diagenetic pyrite with elevated levels of gold. This issue is addressed here, in a preliminary manner, in order to determine the background range of gold in diagenetic pyrite and the "anomalous" range associated with the host rocks to orogenic and Carlin-type deposits. The diagenetic pyrite from three carbonaceous shale units, which are known not be associated with gold mineralization, were studied to compare with the diagenetic pyrite in carbonaceous shales that host the known deposits of Sukhoi Log, northern Carlin Trend, and Bendigo. The background or "barren" carbonaceous shales were selected from three districts: (1) the Paleoproterozoic Barney Creek Formation in the McArthur basin, northern Australia (Bull, 1998), which is the host to stratiform Zn-Pb-Ag mineralization (Large et al., 2005) but not known to host gold mineralization; (2) the Cambrian Alum Shale, Sweden, which is a strongly carbonaceous shale known to host low-grade U-Mo-Ni mineralization but not Au (Leventhal, 1991); and (3) the Mesoproterozoic Rocky Cape Group from the Longback area, western Tasmania (Holm et al., 2003), where carbonaceous shales carry significant diagenetic pyrite but with no known gold occurrences.

LA-ICPMS analyses of diagenetic pyrite from the three gold mineralized districts (Fig. 8A) indicate an invisible gold range from 0.001 to 152 ppm (mean = 1.4 ppm Au) and an arsenic range from 0.7 to 20,400 ppm (mean = 2,550 ppm As). In contrast, the data on carbonaceous shales from the gold-barren districts (Fig. 8B) have a similar range in As contents but a much lower distribution in Au content, from 0.005 to 0.25 ppm Au, with a mean of 0.06 ppm Au. Based on this limited dataset, the boundary between the productive carbonaceous shales and barren carbonaceous shales is suggested to be around 0.25 ppm Au in diagenetic pyrite. This equates to a whole-rock gold content of 5 ppb Au for a carbonaceous shale with 2 wt percent pyrite, which is the estimated average pyrite content of the regional carbonaceous shales investigated in this study.

Our conclusion from this preliminary investigation is that for carbonaceous shales to be a suitable source rock for significant orogenic or Carlin-type deposits, the whole-rock gold content of the shales should be mostly above 5 ppb (or 250 ppb in diagenetic pyrite), with a target mean of 28 ppb in whole rock or 1,400 ppb Au in pyrite. Shales with consistently less than 250 ppb Au in diagenetic pyrite are suggested to be unlikely source rocks for economic gold deposits.

Implications for Exploration

The ideas presented here impact on current models for sediment-hosted Au deposits (e.g., Teal and Jackson, 1997; Phillips and Hughes, 1998; Yeats and Vanderhor, 1998; Bierlein and Crowe, 2000; Hofstra and Cline, 2000) and suggest a somewhat different exploration strategy, especially at the regional to local scale. Some of the characteristics of sedimentary basins and their associated gold ores that have implications for exploration and relate to this sedimentary source-rock model are summarized in Table 4.

Conclusions

The model for sediment-hosted gold deposits presented here differs considerably from current models, particularly in terms of the source of the gold and the two-stage process involved in gold concentration to produce ore grades. It is recognized that one-stage models that depend on a magmatic source or a deep crustal to mantle source are possible, however it is considered that many of the features of the deposits are better explained by the two-stage carbonaceous shale source-rock model. Some of the deposit features that are best explained by this model are summarized as follows:

1. The model explains the ubiquitous Au-As-S relationship in sediment-hosted ores. All three elements are sourced from the carbonaceous shale sediments.
2. The model accounts for the combination of a regional stratigraphic control, with a local structural control on the orebodies. The stratigraphic control indicates the position of stage 1 sedimentary enrichment of gold in the carbonaceous sedimentary package, and the structural control reflects the importance of late diagenetic to metamorphic stage 2 upgrading in producing individual ore shoots (Fig. 17).
3. The model explains why the majority of orogenic deposits are in the chlorite and biotite subfacies of the greenschist facies. These subfacies represent the major metamorphic zones of gold and arsenic release associated with diagenetic pyrite recystallization and ultimate conversion of pyrite to metamorphic pyrrhotite.

TABLE 4. Some Exploration Criteria for Sediment-Hosted Gold Deposits, Relevant to the Carbonaceous Shale Source-Rock Model[1]

A. Tectonic setting	Continental margin basin, developed during ocean anoxic events; early rifting is followed by basin inversion (Carlin type) and basin closure accompanied by metamorpism and deformation (orogenic deposits)
B. Basin lithologic units	Marine siliclastics and/or carbonates and/or volcaniclastics; the sedimentary sequence may vary from proximal to distal turbidites with a high proportion of carbonaceous units
C. Local host rocks	Slope and basin facies are most common host rocks; carbonaceous shales and/or pyritic metalliferous shales, with associated siltstones and sandstones; carbonaceous shales form tops of turbidite cycles
D. Structures	Ore zones are commonly broadly strata bound but crosscutting at local scale; anticlinal fold hinges are the most common mineralized structure; mineralized shear zones, faults and/or breccia zones may cut the folds
E. Metamorphic grade of sedimentary rocks	Varies from very low grade, anchizone (Carlin type) to moderate to high-grade; subgreenshist, greenschist, and amphibolite facies for orogenic deposits; greenschist is the most common facies for orogenic deposits
F. Veining	Laminated-type quartz veins may contain free gold but are not always present; folded saddle reefs are common in anticlinal structures; Carlin-type deposits show silicification but not quartz veining; pyrobitumen veins maybe present in very organic rich sedimentary units
G1. Sulfides-pyrite	Rounded and porous growth forms of diagenetic pyrite in carbonaceous shales may be recrystallized and/or overgrown by euhedral metamorphic-hydrothermal pyrite; diagenetic pyrite is arsenic rich and commonly contains invisible gold at levels exceeding 240 ppb Au and rarely exceeding 10,000 ppb Au; hydrothermal pyrite in many of the medium- to high-grade deposits (e.g., Carlin-type) have very thin Au rich rims of arsenian pyrite, with Au values up to and commonly exceeding 1,000 ppm
G2. Sulfides-pyrrhotite	Microinclusions of pyrrhotite commonly occur in metamorphic pyrites in ores; pyrrhotite may replace pyrite at deeper stratigraphic levels below deposits or within shear zones cutting deposits; the pyrite to pyyrhotite transition zone is a critical zone that indicates widespread release of Au, As, and S from carbonaceous shales to form orogenic deposits, outboard of the transition
G3. Sulfides-other	Arsenopyrite is common in most deposits and may contain significant invisible gold; sphalerite, chalcopyrite, and galena are commonly present as inclusions in metamorphic-hydrothermal pyrite in orogenic deposits
H. Gold-bearing minerals	In subgreenschist facies deposits (e.g., Carlin-type) gold is commonly refractory, occuring either in the structure of arsenian pyrite or as nanoinclusions in arsenian pyrite; some micro- to nanoparticles of gold may also occur in organic matter; at greenschist facies, gold commonly occurs as free gold or electrum grains, in cracks within pyrite or at the margins of pyrite grains; microinclusions in pyrite, of gold telluride phases (enriched in Ag,Pb, Bi), may also be a significant part of the gold resource (e.g., Kumtor); with increasing metamorphic grade, refractory gold in arsenian pyrite, becomes less significant
I. Shale geochemistry	Carbonaceous sedimentary source rocks and host rocks contain variable organic carbon from 0.2 to 20 wt %; they are enriched in V, As, Mo, Ni, Ag, Zn, Cu, Te, Sb, Pb, Hg, Bi, and U; V score = V + Mo + Ni + Zn varies from 250 to over 1,000 ppm; best shale source rocks contain at least 5 ppb gold and may vary up to over 100 ppb; As varies from 10 to over 100 ppm, with mean around 30 to 50 ppm
J. Diagenetic pyrite geochemistry	Favorable source rocks contain diagenetic pyrite enriched in Au, Ag, and As, plus a range of other trace elements including Ni, Co, Mo, Zn, Pb, Cu, Bi, Te, and Se; gold content in diagenetic pyrite is commonly above 250 ppb and may reach several ppm; arsenic mean is around 2,000 ppm with rare pyrite over 1% As; tellurium mean is around 2.5 ppm with a maximum of 100 ppm; Ag/Au is always >1 in diagenetic pyrite
K. Hydrothermal and metamorphic pyrite geochemistry	Metamorphic-hydrothermal pyrite, developed in greenschist facies environments, is commonly depleted in Au, Ag, and other trace elements (except Ni, Co, Se) compared with diagenetic pyrite; proximal (<100 m) to gold ores, the hydrothermal pyrite may exhibit Au-As–enriched rims; in Carlin-type ores thin highly enriched Au-As rims on pyrite are ubiqitous; in orogenic ores, gold maybe concentrated in pyrite cores or pyrite rims or both; Ag/Au is commonly <1 in hydrothermal ore-stage pyrite in both Carlin-type and orogenic deposits
L. Sulfur isotopes	S isotopes in diagenetic pyrite in carbonaceous shale host rocks commonly exhibit a wide range of about 40‰; S isotopes of ore-stage pyrite has a narrower range (<15‰) and a mean value similar to the mean value of the diagenetic pyrite; best ore grades are commonly associated with zones of lower $\delta^{34}S$ in hydrothermal pyrite

[1] Compiled using data from this paper, plus Hofstra and Cline (2000), Emsbo (2000), and Large et al. (2007, 2009, 2010)

4. The model accounts for the typical complex trace element suite, including Mo, V, Ni, Cr, Zn, As, Sb, Hg, Cu, Se, Te, Bi, and W, that is commonly concentrated in carbonaceous shales and also found in these gold deposits.

5. The model explains the reduced seawater sulfate source of the sulfur in the deposits that is revealed by the parallelism between ore pyrite and seawater sulfate sulfur isotope compositions through time (Fig. 14).

However there are many weaknesses and unanswered questions related to the carbonaceous shale source-rock model that require further research, for example, (1) the model does not appear to account for the distribution of sediment-hosted orogenic and Carlin-type deposits along, or adjacent to, major crustal structures or trends; (2) there is a lack of high-quality analytical databases for regional low-level gold and arsenic analyses from black shale sedimentary basins with and without gold deposits; (3) an understanding of the chemistry of carbonaceous shales from different tectonic settings is required in order to put productive basins and deposits within a sedimentary-tectonic framework; (4) a better understanding of how gold is trapped and concentrated in certain types of organic matter is required; (5) data on the partitioning of Au, As, and other trace elements between organic matter, diagenetic

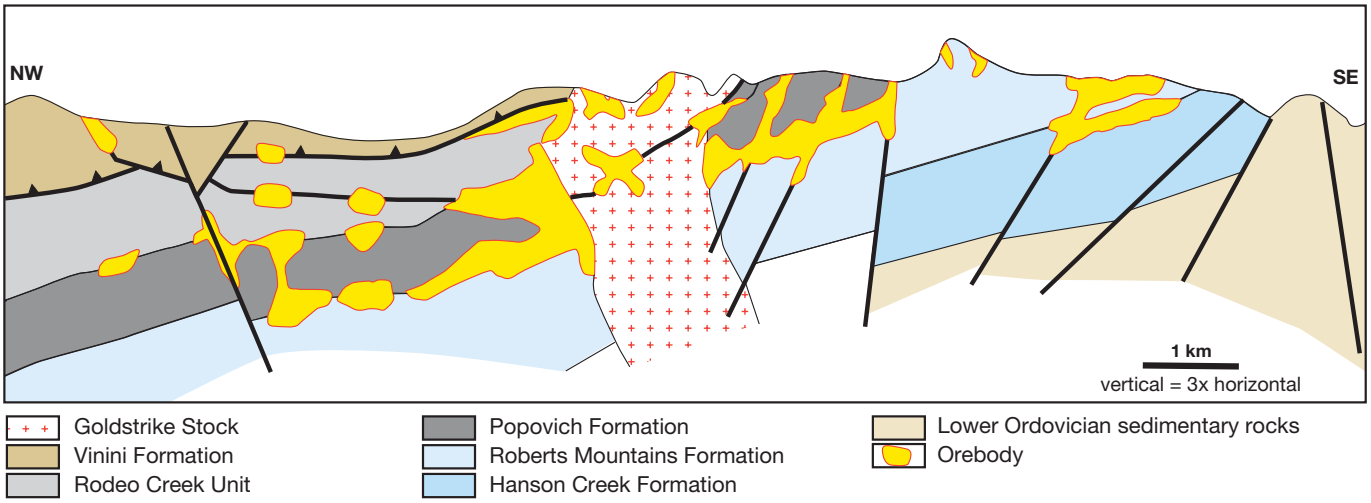

FIG. 17. Regional long section through the northern Carlin Trend, emphasizsing the combination of stratigraphic control and structural control on the siting of gold ores (after Peters, 1996; Hofstra and Cline, 2000).

pyrite, metamorphic pyrite, pyrrhotite, arsenopyrite, and sediment pore fluid would help in further understanding the release of gold from carbonaceous shales during diagenesis and metamorphism.

Acknowledgments

The ideas in this paper were generated during a CODES industry-university collaborative project funded through AMIRA International ("Controls on the Formation and Sulfide Trace Element Signatures of Sediment-Hosted Gold deposits;" P923) that ran from 2005 to 2008. The sponsor companies, Barrick, Newcrest, Newmont, St. Barbara, Perseverance, and Golden Gryphon, are thanked for their support and provision of access to mineral deposits in the Carlin district and Victorian Goldfields. Special thanks to our research colleagues Rob Scott, Poul Emsbo, Leonid Danyushevsky, and Sarah Gilbert for their energetic and critical discussions throughout the course of the project. Jamie Wilkinson is particularly thanked for his critical review of an early draft of the paper. Al Hofstra, Jean Cline, Larry Meinert, and an anonymous reviewer are thanked for their very useful comments that helped to improve the manuscript. Matching funding for this project was provided by the ARC Centre of Excellence program.

REFERENCES

Alegro, T.J., and Maynard, J.B., 2004, Trace-element behaviour and redox facies in core shales of Upper Pennsylvanian Kansas-type cyclothems: Chemical Geology, v. 206, p. 289–318.

Anoshin, G.N., 1977, Gold in magmatic ore deposits: Nauka, Novosibirsk, 206 p.

Anoshin, G.N., Yemel'yanov, E.M., and Perezhogin, G.A., 1969, Gold in the modern sediments of the northern part of the Atlantic Ocean: Geochemistry International, v. 6, p. 897–905.

Arthur, M.A., and Sageman, B.B., 1994, Marine black shales: Depositional mechanisms and environments of ancient deposits: Annual Reviews of Earth and Planetary Sciences, v. 22, p. 499–551.

Bao, Z., 2001, Geochemistry of the sediment-hosted disseminated gold deposits in southwestern Guizhou province, China: Unpublished Ph.D. thesis, Montreal, Canada, University of Quebec, 245 p.

Barley, M.E., and Groves, D.I., 1990, Deciphering the tectonic evolution of Archaean greenstone belts: The importance of contrasting histories to the distribution of mineralization in the Yilgarn craton, Western Australia: Precambrian Research, v. 46, p. 3–20.

Bavinton, O.A., and Keays, R.R., 1978, Precious metal values from interflow sedimentary-rocks from Komatiite sequence at Kambalda, Western Australia: Geochimica et Cosmochimica Acta, v. 42, p. 1151–1163.

Bettles, K., 2002, Exploration and geology, 1962 to 2002, at the Goldstrike property, Carlin Trend, Nevada: Society of Economic Geologists Special Publication 9, p. 275–298.

Bierlein, F.P., and Crowe, D.E., 2000, Phanerozoic orogenic lode gold deposits: Reviews in Economic Geology, v. 13, p. 103–139.

Bortnikov, N.S., Priokof'ev, V.Y., and Razdolina, N.V., 1996, Origin of the Charmitan gold-quartz deposit (Uzbekistan): Geology of Ore Deposits, v. 38, p. 208–226.

Boyle, R.W., 1979, The geochemistry of gold and its deposits: Geological Survey of Canada Bulletin 280, 584 p.

——1986, Gold deposits in turbidite sequences: Their geology, geochemistry and history of the theories of their orogin: Geological Association of Canada Special Paper 32, p. 1–13.

Boyle, R.W., and Jonasson, I.R., 1973, The geochemistry of arsenic and its use as an indicator element in geochemical prospecting: Journal of Geochemical Exploration, v. 2, p. 251–196.

Bull, S.W., 1998, Sedimentology of the Palaeoproterozoic Barney Creek Formation in DDH BMR McArthur 2, southern McArthur basin, Northern Territory: Australian Journal of Earth Sciences, v. 45, p. 21–32.

Burrows, D.R., and Spooner, E.T.C., 1985, Generation of an Archaean H_2O-CO_2 fluid enriched in Au, W and Mo by fractional crystallization in the Mink Lake intrusion, NW Ontario [abs.]: Geological Society of America Abstracts with Programs, v. 17, p. 536.

Buryak, V.A., 1964, The process of regional metamorphism influencing development of gold-sulfide mineralization in the central part of the Lena goldfield: Physical-Chemical Conditions of Magmatism and Metasomatism, All-Union Petrographic Symposium, 3rd, Moscow, Collected Papers, p. 184–189

——1982, Metamorphic processes and ore formation: Moscow, Nedra, 212 p. (in Russian).

Calvert, S.E., and Pedersen, T.F., 1993, Geochemistry of recent oxic and anoxic marine sediments: Implications for the geological record: Marine Geology, v. 113, p. 67–88.

Cas, R.A.F., VandenBerg, A.H.M., Allen, R.L., Clifford, B.A., Fergusson, C.L., Morand, V.J., and Stewart, I.R., 1988, Ordovician: Geological Society of Australia, Victorian Division, p. 63–102.

Chang, Z., Large, R.R., and Maslennikov, V., 2008, Sulfur isotopes in sediment-hosted orogenic gold deposits: Evidence for an early timing and a seawater sulfur source: Geology, v. 36, p. 971–974.

Chappell, B.W., 2010, A chemical database for the New England batholith: New England Orogen Conference, University of New England, Armidale, NSW, Proceedings, p. 119–123.

Chernoff, C.B., and Barton, M.D., 2001, Trace elements in black shale Fe-sulfides during diagenesis and metamorphism: Geological Society of American Annual Meeting, November 5–8, Paper 53.

Cline, J.S., Hofstra, A., Munteau, J., Tosdal, D., and Hickey, K., 2005, Carlin-type gold deposits in Nevada: Critical geologic characteristics and viable models: Economic Geology 100th Anniversary Volume, p. 451–484.

Cook, H.E.., 2005, Carbonate sequence stratigraphy: An exploration tool for sediment-hosted, disseminated gold deposits in the Great Basin: Window to the World, Geological Society of Nevada Symposium, 2005, Reno/Sparks, Nevada, Proceedings, p. 19–24.

Cooke, D.R., Bull, S.W., Large, R.R., and McGoldrick, P.J., 2000, The importance of oxidized brines for the formation of Australian Proterozoic stratiform sediment-hosted Pb-Zn (sedex) deposits: Economic Geology, v. 95, p. 1–18.

Coveney, R.M., Murowchick, J.B., Grauch, R.I., Nansheng, C, and Glascock, M.D., 1992, Field relations, origins and resource implications for platiniferous molybdenum-nickel ores in black shales of South China: Exploration Mining Geology, v. 1, p. 21–28.

Crocket, J.H., 1991, Distribution of gold in the Earth's crust, *in* Foster, R.P., eds., Gold metallogeny and exploration: London, New York, NY, Chapman and Hall, p. 1–36.

Daintree, R., 1866, Report on the geology of the District of Ballan, including remarks on the age and origin of gold: Victorian Geological Survey Report 15, 11 p.

Distler, V.V., Yudovskaya, M.A., Mitrofanov, G.L., Prokof'ev, V.Y., and Lishnevskiy, E.N., 2004, Geology, composition and genesis of the Sukhoi Log noble metals deposit, Russia: Ore Geology Reviews, v. 24, p. 7–44.

Emsbo, P., 2000, Gold in Sedex deposits: Reviews in Economic Geology, v. 13, p. 427–437.

Emsbo, P., and Koenig, A.E., 2005, Discovery and significance of gold-rich bitumen in the Rodeo deposit, northern Carlin Trend, Nevada [abs.]: Geochimica et Cosmochimica Acta, v. 69, suppl., p. A123–A123.

——2007, Transport of Au in petroleum: Evidence from the northern Carlin Trend, Nevada [abs.]: Digging Deeper, Biennial SGA Meeting, 9th, Dublin, Society for Geology Applied to Mineral Deposits, Proceedings p. 695–698.

Emsbo, P., Hutchinson, R.W., Hosftra, A.H., Volk, J.A., Bettles, K.H., Baschuk, G.J., and Johnson, C.A., 1999, Syngenetic Au on the Carlin Trend: Implications for Carlin-type deposits: Geology, v. 27, p. 59–62.

Emsbo, P., Hofstra, A.H., Lauha, E.A., Griffin, G.L., and Hutchinson, R.W., 2003, Origin of high-grade gold ore, source of ore fluid components, and genesis of the Meikle and neighboring Carlin-type deposits, northern Carlin Trend, Nevada: Economic Geology, v. 98, p. 1069–1105.

Ferry, J.M., 1981, Petrology of graphitic sulfide rich schist from south-central Maine: An example of desulfidation during prograde regional metamorphism: American Mineralogist, v. 66, p. 908–931.

Fleet, M.E., Chryssoulis, S.L., Maclean, P.J., Davidson, R., and Weisener, G.G., 1993, Arsenian pyrite from gold deposits—Au and As distribution investigated by SIMS and EMP, and color staining and surface oxidation by XPS and LIMS: Canadian Mineralogist, v. 31, p. 1–17.

Goldberg, I.S., Abramson, G.Y., Haslam, C.O., and Los, V.L., 2007, Depletion and enrichment zones in the Bendigo gold field: A possible source of gold and implications for exploration: Economic Geology, v. 102, p. 745–753.

Goldfarb, R.J., Snee, L.W., Miller, L.D, and Newberry, R.J., 1991, Rapid dewartering of the crust deduced from ages of mesothermal gold deposits: Nature, v. 354, p. 296–299.

Goldfarb, R.J., Miller, L.D., Leach, D.L., and Snee, L.W., 1997, Gold deposits in metamorphic rocks of Alaska: Economic Geology Monograph 9, p. 151–190.

Goldfarb, R.J., Baker, T., Dube, B., Groves, D.I., Hart, C.J.R., and Gosselin, P., 2005, Distribution, character, and genesis of gold deposits in metamorphic terranes: Economic Geology 100th Anniversary Volume, p. 407–450.

Govett, G.J.S., 1983, Rock geochemistry in mineral exploration—Handbook of exploration geochemistry, v. 3: New York, Elsevier, p. 181–225.

Groves, D.I., Goldfarb, R.J., Robert, F., and Hart, C.J.R., 2003, Gold deposits in metamorphic belts: Overview of current understanding, outstanding problems, future research, and significance: Economic Geology, v. 98, p. 1–29.

Helz, G.R., Miller C.V., Charnock, J.M., Mosselmans, J.F.W., Patrick, R.A.D., Garner, C.D., and Vaughan, D.J., 1996, Mechanisms of molybdenum removal from the sea and its concentration in black shales: EXAFS evidence: Geochimica et Cosmochimica Acta, v. 60, p. 3631–3642.

Henderson, P., 1985, Inorganic geochemistry: Moscow, Mir, 277 p.

Henry, G.D., and Boden, D.R., 1997, Eocene magmatism of the Tuscarora volcanic field, Elko County, Nevada, and implications for Carlin-type mineralization: Society of Economic Geologists Guidebook Series, v. 28, p. 193–202.

Hofstra, A.H., and Cline, J.S., 2000, Characteristics and models for Carlin-type gold deposits: Reviews in Economic Geology, v. 13, p. 163–220.

Hofstra, A.H, and Emsbo, P., 2004, Solubility of metals and nutrients in brines: Implications for ore deposits, bioproductivity and anoxia in sedimentary basins [abs.]: Geological Society of America Abstracts, v. 36, p. 200.

——2007, Role of reduced sedimentary rocks in formation of the Great Basin gold province: Implications for exploration in analogous settings: Biennial SGA Meeting, 9th, Dublin, 2007, Proceedings, v. 1, p. 691–694.

Hofstra, A.H., Leventhal, J.S., Northrop, H.R., Landis, G.P., Rye, R.O., Birak, D.J., and Dahl, A.R., 1991, Genesis of sediment-hosted disseminated gold deposits by fluid mixing and sulfidization: Chemical-reaction—path modeling of ore-depositional processes documented in the Jerritt Canyon district, Nevada: Geology, v. 19, p. 36–40.

Hofstra, A.H., Snee, L.W., Rye, R.O., Folger, H.W., Phinisey, J.D., Loranger, R.J., Dahl, A.R., Naeser, C.W., Stein, H.J., and Lewchuk, M.T., 1999, Age constraints on Jerritt Canyon and other Carlin-type gold deposits in the western United States—relationship to mid-Tertiary extension and magmatism: Economic Geology, v. 94, p. 769–802.

Holm, O.H., Crawford, A.J, and Berry, R.F., 2003, Geochemistry and tectonic settings of meta-igneous rocks in the Arthur Lineament and surrounding area, northwest Tasmania: Australian Journal of Earth Sciences, v. 50, p. 903–918.

Hoschek, G., 1984, Alpine metamorphism of calcareous metasediments in the Western Hohe Tauern, Tyrol: Mineral equilibria in COHS fluids: Contributions to Minerallogy and Petrology, v. 87, p. 129–137.

Hu, K., Zhai, J., Liu, Y., Wang, H., Zhang, J., and Jia, R., 2000, Genesis and organic geochemical characteristics of the carbonaceous rock stratabound gold deposits, South China: Science in China, v. 43, p. 507–520.

Hulbert, L.J., Gregoire, D.C., Paktunc, D., and Carne, R.C., 1992, Sedimentary nickel, zinc, and platinum-group-element mineralization in Devonian black shales at the Nick property, Yukon, Canada: A new deposit type: Exploration Mining Geology, v. 1, p. 39–62.

Hulen, J.B., Pinnell, M.L., Neilson, D.L., Cox, J.W., and Blake, J., 1994, The Yankee mine oil occurrence, Alligator Ridge district, Nevada—an exhumed and oxidized, paleogeothermal oil reservoir, *in* Schalla, R.W., and Johnson, E.H., eds., Oil fields of the Great Basin: Nevada Petroleum Society, p. 131–142.

Hutchinson, R.W., 1993, A multi-stage, multi-process genetic hypothesis for greenstonehosted gold lodes: Ore Geology Reviews, v. 8, p. 349–382.

Huyck, H.L.O., 1989, When is a metalliferous black shale, not a black shale?: U.S. Geological Survey Circular 1058, p. 42–56.

Ilchik, R.P, and Barton, M.D., 1997, A amagmatic origin of Carlin-type gold deposits: Economic Geology, v. 92, p. 269–288.

Ilchik, R.P., Brimhall, G.H., and Schull, H.W., 1986, Hydrothermal maturation of indigenous organic matter at the Alligator Ridge gold deposits, Nevada: Economic Geology, v. 81, p. 113–130.

Johnston, M.K., and Ressel, M.W., 2004, Controversies on the origin of world-class gold deposits, Pt. 1: Carlin-type gold deposits in Nevada-Carlin-type and distal disseminated Au-Ag deposits: Related distal expressions of Eocene intrusive centers in north-central Nevada: Society of Economic Geologist Newsletter, v. 59, p. 12–14.

Jory, J., 2002, Stratigraphy and host rock controls of gold deposits of the Northern Carlin Trend: Gold deposits of the Carlin Trend, *in* Thompson, T.B., Teal, L., Meewig, R.O., eds., Nevada Bureau of Miners Geology, Bulletin 111, p. 20–34.

Kashefi, K., Tor, J.M., Nevin, K.P., and Lovley, D.R., 2001, Reductive precipitation of gold by dissimilatory Fe(III)-reducing bacteria and archaea: Applied and Environmental Microbiology, v. 67, p. 3275–3279.

Kazakevich, Y.P., 1971, Lena gold-bearing region, stratigraphy, tectonics, magmatism and occurrences of hard rock gold: Moscow, Nedra Press, 164 p. (in Russian).

Keays, R.R., 1987, Principles of mobilization (dissolution) of metals in mafic and ultramafic rocks—the role of immiscible magmatic sulphides in the generation of hydrothermal gold and volcanogenic massive sulphide deposits: Ore Geology Reviews, v. 2, p. 47–63.

Kerrich, R., 1986, Fluid transport in lineaments: Philosophical Transactions of the Royal Society of London, series A, v. 317, p. 219–251.

Kerrich, R., and Fryer, B.J., 1979, Archaean precious-metal hydrothermal systems, Dome mine, Abitibi greenstone belt: Pt. II. REE and oxygen isotope relations: Canadian Journal of Earth Sciences, v. 16, p. 440–458.

Kerrich, R., Goldfarb, R.J., and Richards, J., 2005, Metallogenic provinces in an evolving geodynamic framework: Economic Geology 100th Anniversary Volume, p. 1097–1136.

Kesler, S.E., Fortuna, J., Ye, Z., Alt, J., C, Core, D.P., Zohar, P., Borhauer, J., and Chryssoulis, S.L., 2003, Evaluation of the role of sulfidation in deposition of gold, Screamer section of the Betze-Post Carlin-type deposit, Nevada: Economic Geology, v. 98, p. 1137–1157.

Ketris, M.P., and Yudovitch, Y.E., 2009, Estimations of Clarkes for Carbonaceous bioliths: World averages for trace element contents in black shales and coals: International Journal of Coal Geology, v. 78, p. 135–148 (doi:10.1016/j.coal.2009.01.002).

Kettler, R.M., Waldo G.S., Penner-Hahn, J.E., Meyers, P.A, and Kesler, S.E., 1990, Sulfidation of organic matter associated with gold mineralization, Pueblo Viejo, Dominican Republic: Applied Geochemistry, v. 5, p. 237–248.

Kribek, B., 1991, Metallogeny, structural, lithological and time controls of ore deposition in anoxic environments: Mineralium Deposita, v. 26, p. 122–131.

Large, R.R., Bull S.W., McGoldrick, P.J., Derrick, G., Carr, G., and Walters, S., 2005, Stratiform and strata-bound Zn-Pb-Ag + Cu deposits of the Proterozoic sedimentary basins of northern Australia: Economic Geology 100th Anniversary Volume, p. 931–963.

Large, R.R., Maslennikov, V., Robert, F., Danyushevsky, L.V., and Chang, Z., 2007, Multistage sedimentary and metamorphic origin of pyrite and gold in the giant Sukhoi Log deposit, Lena gold province, Russia: Economic Geology, v. 102, p. 12331267.

Large, R.R., Danyushevsky, L.V., Hollit, C., Maslennikov, V., Meffre, S., Gilbert, S., Bull, S., Scott, R., Emsbo, P., Thomas, H., and Foster, J., 2009, Gold and trace element zonation in pyrite using a laser imaging technique: Implications for the timing of gold in orogenic and Carlin-style sediment-hosted deposits: Economic Geology, v. 104, p. 635–668.

Large, R.R., Bull, S.W., Scott, R. and Meffre, S., 2010, Stratiform organic-rich V-As-Mo-Se-Ni-Ag-Zn-Au horizons in the Popovich and Roberts Mountain Formations, Carlin district, Nevada [abs.]: Geological Society of Nevada, 2010 Symposium, Reno, Program with Abstracts, p. 59–60.

Large, R.R., Bull, S.W., and Gilbert, S., in press, Multiple syngenetic metalliferous horizons enriched in V, As, Mo, Ni, Ag, Zn, and Au in the northern Carlin Trend: Implications for genesis of world-class gold-arsenic deposits: Geological Society of Nevada, 2010 Symposium, Great Basin Evolution and Metallogeny, Reno, Nevada, p. 1–15.

Layton-Matthews, D., Gemmell, J.B., Large, R.R., and Peter, J., 2008, Trace-element budget of the Que River shale: Exploration implications of hanging-wall modification of sulfide minerals at the Hellyer deposit, Tasmania: International Geological Congress, Oslo 2008, Proceedings, CD -ROM.

Lehmann, B., Nagler, T.F., Holland, H.D., Willie, M., Mao, J., Pan, J., Ma, D.anf Dulski, P., 2007, Highly metalliferous carbonaceous shale and Early Cambrian seawater: Geology, v. 35, p. 403–406.

Leventhal, J., 1991, Comparison of organic geochemistry and in two black shales: Cambrian Alum Shale of Sweden and Devonian Chattanooga Shale of United States: Mineralium Deposita, v. 26, p. 104–112.

Leventhal, J., and Hofstra, A.1990, Characterization of carbon in sediment-hosted disseminated gold deposits, north central Nevada, *in* Hausen, D.M., Halbe, D.N., Petersen, E.U., and Tafuri, W.J., eds., Gold 90: Littleton, CO, Society for Mining, Metallurgy, and Exploration, p. 365–368.

Matti, J.C., and McKee, E.H., 1977, Silurian and Lower Devonian paleogeography of the outer continental shelf of the Cordilleran miogeocline, central Nevada: Paleozoic Paleogeography of the Western United States, SEPM Pacific Coast Paleogeography Symposium 1, Proceedings, p. 181–215.

Meffre, S., Large, R.R., Scott, R., Woodhead, J., Chang, Z., Gilbert, S.E., Danyushevsky, L.V., Maslennikov, V., and Hergt, J., 2008, Age and pyrite Pb-isotopic composition of the giant Sukhoi Log sediment-hosted gold deposit, Russia: Geochimica et Cosmochimica Acta, v. 72, p. 2377–2391.

Mumin, A.H., Fleet, M.E., and Chryssoulis, S.L., 1994, Gold mineralisation in As-rich mesothermal gold ores of the Bogosu-Prestea mining district of the Ashanti gold belt, Ghana: Remobalization of "invisible" gold: Mineralium Deposita, v. 29, p. 445–460.

Muntean, J., Cline, J, Simon, A., and Long, A., 2011, Magmatic-hydrothermal origin of Nevada's Carlin-type gold deposits: Nature Geoscience, v. 4, p. 122–127.

Nekrasov, I.Y., 1996, Geochemistry, mineralogy and genesis of gold deposits: Rotterdam, A.A.Balkema, 329 p.

Nifontov, R.V., 1961, A new principle of placer classification: Mineral, Syr'e, no. 2, p. 10–21.

Nutt, C.J., and Hofstra, A.H., 2007, Bald Mountain gold mining district, Nevada: A Jurassic reduced intrusion-related gold system: Economic Geology, v. 102, p. 1129–1155.

Perring, C.S., Groves, D.I., and Ho, S.E., 1987, Constraints on the source of auriferous fluids for Archaean gold deposits: Geology Department and Extension Service, University of Western Australia Publication 11, p. 287–306.

Perring, C.S., Groves, D.I., and Shellabear, J.N., 1991, The geochemistry of Archean gold ores from the Yilgarn block of Western Australia: Implications for gold metallogeny: Minerals and Energy Research Institute of Western Australia Report 82, 15 p.

Peters, S.G., 1996, Definition of the Carlin Trend using orientation of fold axes and application to ore control and zoning in the Central Betze orebody, Betze-Post mine, *in* Green, S,M., and Strusacker, E., eds., Geology and ore deposits of the American Cordillera. Field Trip Guidebook Compendium: Reno, Geological Society of Nevada, p. 203–240.

Phillips, G.N., and Groves, D.I., 1983, The Nature of Archean gold-bearing fluids as deduced from gold deposits of Western Australia: Journal of the Geological Society of Australia, v. 30, p. 25–39.

Phillips, G.N., and Hughes, M.J., 1998, Victorian gold deposits: AGSO Journal of Australian Geology and Geophysics v. 17, p. 213–216.

Phillips, G.N., Groves, D.I., and Brown, I.J., 1987, Source requirements for the Golden Mile, Kalgoolie: Significance to the metamorphic replacement model for Archean gold deposits: Canadian Journal of Earth Sciences, v. 24, p. 1643–1651.

Pitcairn, I.K., Teagle, D.A.H., Craw, D., Olivo, G.K., Kerrich, R., and Brewer.T.S, 2006, Sources of metals and fluids in orogenic gold deposits; Insights from the Otago and Alpine schists, New Zealand: Economic Geology, v. 101, p. 1525–1546.

Procenko, V.F., 2008, Metamorphism and ore genesisin black shale units of Central Asia: Tashkent State Enterprises: Institute of Mineral Resources, 116 p. (in Russian).

Quinby-Hunt, M.S., and Wilde, P., 1993, Thermodynamic zonation in the black shale facies based on iron-maganese-vanadium content: Chemical Geology, v. 113, p. 297–317.

Quinby-Hunt, M.S., Wide, P., and Berry, W.B.N., 1989a, Element geochemistry of low calcic black shales—statistical comparison with other shales: U.S Geological Survey Circular 1037, p. 8–15.

Radtke, A.S., 1985, Geology of the Carlin gold deposit, Nevada: U.S. Geological Survey Professional Paper 1267, 124 p.

Razvozzhaeva, E.A., Prokof'ev, V.Y., Spiridonov, A.M., Martikhaev, D.K., and Prokopchuk, S.I., 2002, Precious metals and carbonaceous substances in ores of the Sukhoi Log deposit, eastern Siberia, Russia: Geology of Ore Deposits, v. 44, p. 103–111.

Razvozzhaeva, E.A., Nemerov, V., Spiridonov, A.M., and Prokopchuk, S.I., 2008, Carbonaceous substance of the Sukhoi Log gold deposit (East Siberia): Russian Geology and Geophysics, v. 49, p. 371–377.

Reich, M., Kesler, S.E., Utsunomiya, S., Palenik, C.S., Chryssoulis, S.L., and Ewing, R., 2005, Solubility of gold in arsenian pyrite: Geochemica et Cosmochimica Acta, v. 69, p. 2781–2796.

Reimann, C., and de Caritat, P., 1998, Chemical elements in the environment: Fact sheets for the geochemist and environmental scientist: Berlin, Springer, 398 p.

Ressel, M.W., Nobel, D.C., Henry, C.D., and Trudel, W.S., 2000, Dike-hosted ores or the Beast deposit and importance of Eocene magmatism in gold mineralization of the Carlin Trend, Nevada: Economic Geology, v. 95, p. 1417–1444.

Reznik, V.P, and Fedoronchuk, N.A., 2000, Microscopic gold in marine and oceanic sediments: Lithology and Mineral Resources, v. 35, p. 311–318.

Rimmer, S.M., 2004, Geochemical paleoredox indicators in Devonian-Mississippian black shales, Central Appalachian Basin, USA: Chemical Geology, v. 206, p. 373–391.

Ryan, R.J., and Smith, P.K., 1998, A review of the mesothermal gold deposits of the Meguma Group, Nova Scotia, Canada: Ore Geology Reviews, v. 13, p. 153–183.

Scott, R.J., Large, R.R., Emsbo, P., and Bull, S.W., 2008, Carlin district pyrite trace element characterisation—summary of major findings in AMIRA P923: Controls on the formation and sulfide trace element signatures of sediment-hosted gold deposits: AMIRA P923 Final Data Compilation, CODES, University of Tasmania, 39 p.

Seedorff, F., 1991, Magmatism, extension, and ore deposits of Eocene to Holocene age in the Great Basin: Mutual effects and preliminary genetic relationships: Geology and Ore Deposits of the Great Basin Symposium, Geological Society of Nevada, Reno, Nevada, Proceedings, p. 133–178.

Sillitoe, R.H., and Bonham, H.F., 1990, Sediment-hosted gold deposits: Distal products of magmatic-hydrothermal systems: Geology, v. 18, p. 157–161.

Shpirt, M.Ya., Punanova, S.A, and Strizhakova, Yu.A., 2007, Trace elements in black and oil shales: Solid Fuel Chemistry, v. 41, p119–127.
Spooner, E.T.C., 1993, Magmatic sulphide/volatile interaction as a mechanism for producing chalcophile element enriched, Archean Au-quartz, eqithermal Au-Ag and Au skarn hydrothermal ore fluids: Ore Geology Reviews, v. 7, p. 359–379.
Strauss, H., 2006, Anoxia through time: Reviews of Geophysics, v. 33, p. 241–265.
Taylor, S.R., and McLennan, S.M., 1995, The geochemical evolution of the continental crust: Reviews of Geophysics, v. 33, p. 241–265.
Teal, L., and Jackson, M., 1997, Geologic overview of the Carlin Trend gold deposits and descriptions of recent deep discoveries: Society of Economic Geologists Newsletter 31, p. 1, 13–25.
Thomas, H.V., Large R.R., Bull, S.W., Maslennekov, V.V., Berry, R.F., Fraser, R., Froud, S, and Moye, R., 2011, Pyrite and pyrrhotite textures and composition in sedimentary rocks, laminated quartz veins, and gold reefs at the Bendigo mine, Australia: Insights for ore genesis: Economic Geology, v. 106, p. 1–31.
Thompson, J.F.H., Sillitoe, R.H., Baker, T., Lang, J.R., and Mortensen, J.K., 1999, Intrusion-related gold deposits associated with tungsten-tin procinces: Mineralium Deposita, v. 34, p. 232–334.
Titley, S.R., 1991, Phanerozoic ocean cycles and sedimentary-rock-hosted gold ores: Geology, v. 19, p. 645–648.
Tomkins A.G., 2010, Windows of metamorphic sulfur liberation in the crust: Implications for gold deposit genesis: Geochimica et Cosmochimica Acta, v. 74, p. 3246–3259.
Tomkins A.G, and Grundy C., 2009, Upper temperature limits of orogenic gold deposit formation: Constraints from the granulite-hosted Griffin's Find deposit, Yilgarn craton: Economic Geology, v. 104, p. 669–685.
Tribovillard, N., Algeo, T.J., Lyons, T., and Riboulleau, A., 2006, Trace metals as paleoredox and paleoproductivity proxies: An update: Chemical Geology, v. 232, p. 12–32.
Turner, S.P., Kelley, S.P., VandenBerg, A.H.M., Foden, J.D., Sandiford, M., and Floettmann, T., 1996, Source of the Lachlan fold belt flysch linked to convective removal of the lithospheric mantle and rapid exhumation of the Delamerian-Ross fold belt: Geology, v. 24, p. 941–944.
Vilor, N.V., 1983, Gold in black shales: Geochemistry International, v. 20, p. 167–177.
Wedepohl, K.H., 1995, The composition of the continental crust: Geochimica et Cosmochimica Acta, v. 59, p. 1217–1232.
Williams-Jones, A.E., and Migdisov, A.A., 2007, The solubility of gold in crude oil: Implications for ore genesis [abs.]: Digging Deeper, Biennial SGA Meeting, 9th, Dublin, Society for Geology Applied to Mineral Deposits, Proceedings p. 765–768.
Willman, C.E., 2007, Regional structural controls of gold mineralization, Bendigo and Castlemaine goldfields, central Victoria, Australia: Mineralium Deposita, v. 42, p. 449–463.
Willman, C.E., Korsch, R.J., Moore, D.H., Cayley, V.A., Lisitsin, T.J., Rawling, T.J., Morand, V.j, and O'Shea, P.J., 2010, Crustal-scale fluid pathways and source rocks in the Victorian gold province, Australia: Insights from deep seismic reflection profiles: Economic Geology, v. 105, p. 895–915.
Wood, B.L., and Large, R.R., 2007, Syngenetic gold in western Victoria: Occurrence, age and dimensions: Australian Journal of Earth Sciences, v. 54, p. 711–732.
Wood, B.L., and Popov, N.P., 2006, The giant Sukhoi Log deposit, Siberia: Russian Geology and Geophysics, v. 47, p. 315–341.
Wood, S.A., 1996, The role of humic substances in the transport and fixation of metals of economic interest (Au, Pt, Pd, U, V): Ore Geology Reviews, v. 11, p. 1–33.
Yeats, C.J., and Vanderhor, F., 1998, Archaean lode-gold deposits: AGSO Journal of Australian Geology and Geophysics, v. 17, p. 253–258.
Zhang, A., Pan, Y., and Weng, C., 1995, The organic geochemistry of auriferous black shales, *in* Pasava, J., Kribek, B., and Zak, K., eds., Mineral deposits: From their origin to their environmental impacts: Prague, Czech Republic, Society for Geology Applied to Mineral Deposits, p. 829–831.
Zhang, J., Lu J., Zhai J, and Fan Y., 1997, Simulating experiments on enrichment of gold by bacteria and their geochemical significance: Chinese Journal of Geochemistry, v. 16, no. 4, p. 369–373.

TABLE A1. LA-ICPMS Analyses of Selected Gold-Bearing Diagenetic Pyrite and Organic Matrix in Carbonaceous Shales from Sukhoi Log, Bendigo, Spanish Mountain, Northern Carlin Trend, and Alum Shale

Sample no.	Analysis no.	Mineral	Au (ppm)	As (ppm)	Ag (ppm)	Ag/Au	Al (ppm)	Ti (ppm)	V (ppm)	Cr (ppm)	Mn (ppm)	Fe internal standard	Co (ppm)	Ni (ppm)	Cu (ppm)
Sukhoi Log															
SL-1-98.5a	FE09A26	Pyrite	0.57	582.9	5.2	9.1	6607.9	57.6	8.3	10.2	73.2	453000.0	144.8	148.1	34.5
SL-1-91a	FE09A13	Pyrite	0.70	719.0	7.1	10.1	7338.9	102.5	11.0	8.8	80.7	453000.0	190.5	209.5	40.2
524/70.9-1-3	AP04A73	Pyrite	1.82	2656.7	16.6	9.1	6071.9	49.4	7.2	6.9	22.4	465000.0	177.1	758.9	123.6
156/526-10	MA23A84	Pyrite	6.18	3601.5	12.8	2.1	9246.4	291.8	46.0	21.2	306.9	465000.0	175.5	1021.4	228.0
156/225-C1-9	MA14A11	Pyrite	6.55	3273.9	16.4	2.5	4066.0	48.9	6.0	10.7	1969.2	465000.0	170.8	1252.2	595.0
156/225-C2-1 fram	MA14A13	Pyrite	7.41	2902.2	15.5	2.1	16171.1	159.6	22.6	26.2	1440.1	465000.0	263.8	1488.4	479.9
524/68.5-NC-2	AP04A94	Pyrite	5.02	3043.6	14.0	2.8	29315.2	174.6	45.8	44.0	256.1	465000.0	2016.5	1023.1	302.2
176/300-19	MA23A49	Pyrite	7.47	1425.2	10.8	1.4	21692.8	178.9	68.8	83.4	270.6	465000.0	150.4	598.6	328.2
Bendigo															
NBD171-377.7B-6	AP18A18	Pyrite	0.76	635.2	15.3	20.2	1896.4	48.1	4.5	6.4	7.3	465000.0	89.0	1858.5	3304.1
NBD171-377.7B-7	AP18A19	Pyrite	0.26	446.8	7.2	27.5	318.6	27.1	0.7	1.2	1.2	465000.0	28.2	1704.5	2519.0
NBD171-377.7B-8	AP18A20	Pyrite	0.70	1865.5	14.7	21.0	2468.0	164.0	5.6	8.3	3.4	465000.0	238.9	2771.5	3725.7
NBD161-454.3 C2-3	AP08A43	Pyrite	1.62	3954.7	0.4	0.2	15027.3	1752.8	31.1	79.4	47.3	465000.0	767.2	893.6	40.7
NBD161-437.15-C2-4	AP02A42	Pyrite	1.45	840.5	1.2	0.8	25620.5	1150.4	33.9	75.9	104.4	465000.0	3119.0	610.7	119.9
Spanish Mountain															
SM1-79.8-A-8	JA17B09	Pyrite	3.85	11606.6	24.8	6.5	556.9	221.7	1.7	<3.09	3.4	465000.0	11.2	2896.3	2262.0
SM1-79.8-B-1	JA17B15	Pyrite	9.51	11180.5	10.1	1.1	157.6	13.9	0.7	<3.09	<1.32	465000.0	28.0	2828.0	584.8
SM1-79.8-A-9	JA17B07	Pyrite	10.69	11393.2	21.9	2.0	313.4	217.5	0.8	<3.09	1.6	465000.0	2.9	88.4	1601.8
SM1-79.8-A-9a	JA17B08	Pyrite	10.82	12718.1	15.1	1.4	1177.6	83.9	4.2	<29.33	<9.67	465000.0	<3.38	26.5	1222.0
SM1-79.8-B-L6	JA17B05	Pyrite	10.02	13968.6	8.6	0.9	789.9	62.3	7.0	4.5	<1.32	465000.0	17.9	3095.2	708.7
SM1-79.8-A-L12	JA17B03	Pyrite	4.54	5908.5	40.1	8.8	2011.8	419.6	5.5	9.4	5.8	465000.0	46.9	2003.7	2541.5
Northern Carlin Trend															
225-1-1	AU21A03	Pyrite	10.60	2454.7	148.0	14.0	1950.4	269.5	2691.6	1185.4	168.8	465000.0	16.5	9601.4	12458.1
225-4-2	AU21A06	Pyrite	72.35	3896.5	174.7	2.4	3768.5	113.9	2169.8	1140.2	303.1	465000.0	12.7	8946.2	12590.3
225-9-2	AU21A12	Pyrite	168.71	5623.4	343.1	2.0	10488.6	145.0	4542.5	437.8	891.2	465000.0	2.9	2987.6	2301.2
225-15-1	AU21A22	Pyrite	15.78	2085.4	112.6	7.1	2895.7	649.0	3320.9	1056.6	235.5	465000.0	4.9	3885.6	11232.4
224-2-1	AU21A28	Pyrite	9.54	3282.3	242.7	25.4	5780.4	103.3	859.2	263.6	831.0	465000.0	6.8	3667.6	3502.3
224-3-2	AU21A32	Pyrite	20.28	6575.1	219.1	10.8	6922.8	82.0	1843.8	381.6	1039.8	465000.0	4.3	1169.4	865.1
224-7-4	AU21A41	Pyrite	16.37	3629.9	212.1	13.0	485.5	36.3	883.0	524.0	480.6	465000.0	18.5	8035.6	10290.8
CD13c-2524.6	OC16A124	Organic matter	4.55	55498.7	2.4	0.5	409.9	5358.9	1739.9	979.2	4.7	100.0	<1	290.8	<20
CD13c-2524.6	OC16A125	Organic matter	1.95	75716.8	2.3	1.2	307.7	3642.2	1357.0	650.8	<2	100.0	<1	225.2	<11
Alum shale															
Alum-4-C1-01	AU08A03	Pyrite	0.13	3663.7	307.8	2448.3	485.9	30.8	31.7	<25.674	4136.2	465000.0	7.0	495.9	2223.9
Alum-4-C1-02	AU08A04	Pyrite	0.11	3384.1	227.2	2011.9	12.0	3.7	17.8	<25.674	2498.5	465000.0	7.6	1578.5	5302.2
Alum-4-C1-03	AU08A05	Pyrite	0.11	3028.9	218.0	1947.4	184.0	47.6	31.4	<25.674	2996.8	465000.0	5.4	527.6	190.3
Alum-4-C1-04	AU08A06	Pyrite	0.11	2949.7	154.5	1421.5	830.2	141.1	60.0	<21.167	1016.8	465000.0	137.6	5762.8	1080.7
Alum-4-C2-01	AU08A15	Pyrite	0.07	3115.7	94.4	1321.9	5908.7	354.4	298.3	51.1	1537.5	465000.0	73.1	1829.3	3296.4
Alum-4-C2-02	AU08A16	Pyrite	0.07	2449.7	122.9	1888.0	266.7	13.0	18.5	<21.167	928.5	465000.0	106.5	7936.7	1705.8
Alum-4-C2-03	AU08A17	Pyrite	0.06	2165.1	120.9	2089.0	1001.0	81.3	63.6	<21.167	1074.7	465000.0	52.1	5980.7	191.7
Alum-4-C2-04	AU08A18	Pyrite	0.04	1755.7	95.8	2434.4	1166.9	111.6	62.0	14.6	1798.8	465000.0	8.8	321.9	273.2
Alum-4-C2-05	AU08A19	Pyrite	0.04	1728.8	67.1	1746.6	1452.5	55.7	59.7	10.5	1140.2	465000.0	42.7	4221.6	433.3

TABLE A1. *(Cont.)*

Sample no.	Zn (ppm)	Se (ppm)	Mo (ppm)	Ag (ppm)	Sn (ppm)	Sb (ppm)	Te (ppm)	Ba (ppm)	La (ppm)	W (ppm)	Tl (ppm)	Pb (ppm)	Bi (ppm)	Th (ppm)	U (ppm)
Sukhoi Log															
SL-1-98.5a	113.4	2.8	0.7	5.2	0.5	75.8	0.4	22.2	0.0	0.2	0.5	181.9	3.5	2.0	3.3
SL-1-91a	136.5	4.7	1.1	7.1	1.2	90.9	1.7	29.3	0.0	0.3	0.4	298.5	5.2	0.3	1.0
524/70.9-1-3	6.2	37.3	1.4	16.6	1.4	17.0	<1.48	86.3	<0.02	0.4	0.1	232.4	7.1	<0.01	0.0
156/526-10	90.5	22.3	7.3	12.8	0.5	43.1	<9.28	85.7	<0.18	<0.38	0.3	441.5	7.1	<0.07	0.4
156/225-C1-9	47.6	4.0	30.3	16.4	1.6	77.7	<2.12	87.7	0.1	0.3	0.3	612.2	9.1	<0.02	0.0
156/225-C2-1 fram	53.1	4.0	28.7	15.5	3.7	86.8	2.5	163.4	0.1	0.9	0.5	678.3	8.2	0.1	0.1
524/68.5-NC-2	36.1	4.0	0.5	14.0	0.5	73.8	<16.44	668.6	4.5	<1.14	0.6	590.6	20.1	0.2	0.5
176/300-19	69.2	45.4	29.4	10.8	2.0	39.0	<2.95	518.6	0.6	0.7	0.3	560.8	5.0	<0.05	2.4
Bendigo															
NBD171-377.7B-6	48.7	71.8	31.2	15.3	0.4	160.3	7.2	19.6	0.0	0.0	0.1	2848.7	85.6	0.1	0.0
NBD171-377.7B-7	31.6	76.5	3.8	7.2	0.3	31.0	2.1	4.3	0.0	0.0	0.0	1423.3	23.4	0.0	0.0
NBD171-377.7B-8	53.9	91.1	21.3	14.7	0.6	168.9	11.7	24.2	0.5	0.2	0.1	4118.5	105.1	0.0	0.0
NBD161-454.3 C2-3	21.5	30.6	59.8	0.4	1.0	170.2	1.0	104.1	22.1	3.9	1.0	310.8	179.1	3.5	0.8
NBD161-437.15-C2-4	69.9	69.4	13.9	1.2	1.7	415.4	7.7	141.1	0.2	2.0	1.8	982.0	275.4	12.5	9.7
Spanish Mountain															
SM1-79.8-A-8	156.5	95.0	3.7	24.8	<0.28	8.2	0.9	7.9	2.2	5.5	<0.03	630.4	0.3	4.9	1.7
SM1-79.8-B-1	234.3	108.3	<0.82	10.1	<0.28	3.5	1.6	4.3	<0.01	<0.09	<0.03	214.4	0.1	<0.02	<0.01
SM1-79.8-A-9	138.4	97.0	4.0	21.9	<0.28	5.0	1.6	3.3	0.6	13.1	<0.03	93.0	0.0	0.6	0.3
SM1-79.8-A-9a	31.6	115.0	<6.95	15.1	<2.88	9.3	<5.95	27.5	<0.09	4.2	<0.28	432.2	<0.17	1.8	1.1
SM1-79.8-B-L6	38.3	77.0	<0.82	8.6	<0.28	1.9	<0.71	18.6	0.0	<0.09	0.0	181.8	0.1	1.2	0.4
SM1-79.8-A-L12	195.1	96.5	<0.82	40.1	0.5	12.9	1.3	8.1	7.5	27.5	<0.03	166.2	0.1	1.6	0.6
Northern Carlin Trend															
225-1-1	179.4	3561.2	740.8	148.0	6.7	671.2	11.9	32.5	0.2	1.3	246.4	332.2	4.7	0.1	1.3
225-4-2	1088.9	3992.5	2657.2	174.7	4.2	822.9	14.2	37.9	1.4	16.2	291.0	433.0	4.9	0.3	3.5
225-9-2	1333.2	4248.4	1014.1	343.1	5.8	1239.9	13.5	47.3	0.2	3.0	370.6	577.0	2.3	<0.19	1.3
225-15-1	132.8	3081.1	452.7	112.6	2.6	531.5	10.8	30.0	5.3	2.0	181.5	265.6	4.5	1.5	1.8
224-2-1	974.0	2734.6	1269.5	242.7	9.4	861.0	13.0	56.8	3.3	3.1	263.0	340.6	2.6	0.3	34.6
224-3-2	3409.9	3300.5	1085.6	219.1	15.4	971.5	9.8	50.3	2.3	2.7	253.5	333.4	1.4	0.4	3.1
224-7-4	255.0	3192.0	1545.4	212.1	0.6	1122.0	16.7	28.9	0.3	1.6	416.3	448.0	5.6	0.1	0.9
CD13c-2524.6	32.7	94.6	689.8	2.4	<4.3	400.5	1.5	155.9	11.6	1.7	4.2	15.7	0.1	46.5	424.5
CD13c-2524.6	<4	145.1	440.2	2.3	<2.4	135.9	<1	89.8	7.0	1.5	3.4	9.5	0.1	31.6	246.7
Alum shale															
Alum-4-C1-01	48.6	298.8	297.1	307.8	<0.311	156.3	15.2	78.6	0.2	<0.137	441.6	104.0	0.4	<0.054	1.2
Alum-4-C1-02	103.3	261.9	608.0	227.2	<0.311	133.0	23.6	74.3	<0.027	0.2	368.3	132.5	0.6	<0.054	0.0
Alum-4-C1-03	32.8	257.7	353.7	218.0	<0.311	115.7	14.8	52.6	0.1	<0.137	268.0	48.2	0.3	<0.054	1.1
Alum-4-C1-04	30.2	199.6	108.6	154.5	<0.227	100.9	3.7	21.8	0.1	<0.149	101.3	28.3	0.6	0.1	2.4
Alum-4-C2-01	29.6	224.7	310.9	94.4	<0.311	111.6	7.7	61.1	2.6	0.4	149.5	227.1	1.1	1.7	24.2
Alum-4-C2-02	296.8	147.9	69.9	122.9	<0.227	69.9	2.4	24.1	0.1	<0.149	81.9	47.2	0.5	0.1	1.1
Alum-4-C2-03	251.0	144.3	83.8	120.9	0.3	91.1	2.6	18.8	<0.029	<0.149	69.0	41.1	0.6	0.3	3.1
Alum-4-C2-04	22.8	122.5	333.5	95.8	0.1	65.7	5.6	43.2	0.4	0.2	125.6	63.2	0.3	0.2	3.3
Alum-4-C2-05	796.3	137.5	186.2	67.1	0.2	55.8	3.3	22.4	0.1	0.0	74.5	42.2	0.4	0.4	3.4